E3ANT

A Matlab Package for Phased Array Beam Shape Inspection
Version 1.0

J Markkanen
www.sgo.fi/~jussi/

September 22, 2006

Contents

List of Figures

1. Introduction

These notes are a work on progress. They were started to document a set of Matlab functions, the E3ANT package, which I wrote to simulate the beam shape of a phased array for the EISCAT 3D project. When starting the work, I knew absolutely nothing about phased arrays, and had to start digging up. It turned out that the books I could place my hands on where difficult for me to understand, or did not handle the aspects I was interested in, so I started to re-inventing the wheel for myself. These notes grew up in an effort to write down, in self-contained manner, what I have learned so far, and especially, what I have found puzzling.

What I most especially have been struggling to understand is the supposedly well known equality of gain in reception and transmission. I'm getting to the impression that this is one of the things in physics that has been clarified so early in history that it now considered to use the result in all possible situations without any further justification. And, like in the case of, say, Heisenberg's uncertainly relation, the actual meaning of the result and its original premises, are getting lost in the fog of history. Few books nowadays seem to bother to prove the results, and even those that do, still refer, without proof, to even more basic results of electromagnetism. So it is actually quite difficult to be sure that the premises on which the result is based actually hold on the E3D situation.

The premises normally involve a single antenna used on-line in transmission and reception. I think I understand that situation and have traced the derivation in these notes. But what I'm actually worried about is what happens in the E3D situation when the beam-forming is done off-line and in possibly multiple ways. How do we compute the gain then, what is the equivalent antenna(s) for all those beams? I do not know, yet.

I start in the next section by spectral domain based presentation of the basic ideas of array beam steering, with the main aim being in understanding the difference between time-steering and phase-steering.

In chapter 3 I labour on the issue of antenna gain, especially, the relation between the reception gain and the transmission gain. Also, I dwell on the, to me counterintuitive, result that the array gain can be larger (or smaller) than the "natural" value, element gain times the number of elements.

In Chapter 4 I derive the equations needed to compute array gain in absolute terms, especially, the power integral.

In chapter 5 I consider the effect of timing accuracy to the pointing accuracy, though it now appears that my underlying assumptions about the planned array might not be relevant anymore. Also, my timing error simulations, presented in chapter 6, have been rendered irrelevant by the much more careful computations done by Gustav Johansson and others of the Luleå group.

In chapter 7 I compute estimates for the SNR of the Kiruna test array.

The figures for these notes are in a section of their own, starting on p. 34. The blue-coloured references to figures, equations, page numbers, sections, etc, in the on-line PDF version of this document are clickable hyperlinks. They should work in the Adobe Acrobat Reader, and the Preview application on Mac OS X.

2. Time steering and phase steering

2.1. Time steering

In general, an incoming wave field can be represented by

$$s(t,\mathbf{r}) = \int d^3\mathbf{k}\, S(\mathbf{k}) \mathrm{e}^{i\,(\mathbf{k}\cdot\mathbf{r}-\omega_{\mathbf{k}}t)}\,, \tag{1}$$

where

$$\omega_{\mathbf{k}} = \|\mathbf{k}\|c\,. \tag{2}$$

As a special case, a multifrequency wave ("wave packed", "pulse") coming from the direction of the unit vector $\hat{\mathbf{u}}$ is decomposed to plane waves as

$$s(t,\mathbf{r};\hat{\mathbf{u}}) = \int d\omega\, S_{\hat{\mathbf{u}}}(\omega) \mathrm{e}^{i(\frac{\omega}{c}\hat{\mathbf{u}}\cdot\mathbf{r}-\omega t)} \tag{3}$$

Assume the M array elements are at positions $\mathbf{R}_m$, and denote by $s_m(t)$ the signal voltage across the terminal of the element m. The elements take spatial samples of the incoming wavefield,

$$s_m(t) = a_m\, s(t,\mathbf{R}_m)\,, \tag{4}$$

where a_m is a real-valued non-negative amplification factor, which can be used to implement non-trivial "window functions" on the array. Next, time-steer the array by delaying the signals s_m by an element-wise delay T_m,

$$T_m = \frac{\mathbf{R}_m\cdot\hat{\mathbf{u}}_0}{c}\,. \tag{5}$$

At the moment consider the unit vector $\hat{\mathbf{u}}_0$ just a parameter that quantifies the scanning. We'll verify later that $\hat{\mathbf{u}}_0$ is the direction of the scanned beam. But we note already here that T_m is the amount of time by which the incoming wave front from direction $\hat{\mathbf{u}}_0$ hits later the element at $\mathbf{R}_m$ than it hits the coordinate system's origin $\mathbf{R}=\mathbf{0}$.

After the delays, an adder combines the elementary signals, to the final beam-formed signal

$$z = z(t,\hat{\mathbf{u}};\hat{\mathbf{u}}_0) = \sum s_m(t-T_m)\,. \tag{6}$$

In the notation of Eq. (6), we included explicitly the two unit vectors $\hat{\mathbf{u}}$ and $\hat{\mathbf{u}}_0$, to keep the definition of the signal $z(t)$ in Eq. (6) as clear as possible: $z(t)$ is the signal voltage generated by a pulse coming from direction $\hat{\mathbf{u}}$ when the array has been scanned to direction $\hat{\mathbf{u}}_0$. But this description begs the following question: shouldn't the voltage $z(t)$ at the beam former output somehow also depend on what actually is on the sky? Of course it does depend: If the *only* target on the sky is a point target in the direction $\hat{\mathbf{u}}$ (yes: $\hat{\mathbf{u}}$, not $\hat{\mathbf{u}}_0$) , the signal z in Eq. (6) gives the actual measured voltage. But in general, there are more targets, a large distributed soft target in the EISCAT case. Then the actual signal voltage is a sum integral over all directions, and we should compute $z(t)$ using Eq. (1) throughout, instead of Eq. (3). The other way, which we will adopt in this note , is to continue using Eq. (3), but to keep in mind that Eq. (6) does not give the total signal, but only the linearly additive contribution, or "weight", of the target in the direction $\hat{\mathbf{u}}$ to the total observed signal. We will see that the in practice only a narrow cone around the direction of $\hat{\mathbf{u}}_0$, and its direction-aliased directions if any, contribute to the sum effectively.

We will first show that as a function of $\hat{\mathbf{u}}$, $z(t)$ is "maximized" in the direction of $\hat{\mathbf{u}}_0$ so that the parameter $\hat{\mathbf{u}}_0$ indeed is the beam-steering direction as we have been saying. And we verify that *in that direction* there is no dispersion, that is, all the frequency components of the pulse yield exactly the same, equally phased, contribution to the sum, and hence the temporal shape of the incoming signal is recovered without distortion. On the other hand, there is dispersion in non-center-of-the-beam directions. The effect hopefully is insignificant for narrow beams, but perhaps we should make sure. (Question: Does GJ's system simulation already do this?) Expanding Eq. (6) we get

$$z(t,\hat{\mathbf{u}};\hat{\mathbf{u}}_0)=\sum_m a_m\int d\omega\, S_{\hat{\mathbf{u}}}(\omega)\mathrm{e}^{i\omega[(\hat{\mathbf{u}}-\hat{\mathbf{u}}_0)\cdot\frac{\mathbf{R}_m}{c}-t]}\,, \tag{7}$$

so that in the direction $\hat{\mathbf{u}}=\hat{\mathbf{u}}_0$ we have

$$z(t,\hat{\mathbf{u}}_0;\hat{\mathbf{u}}_0)=\sum_m a_m\int d\omega\, S_{\hat{\mathbf{u}}_0}(\omega)\mathrm{e}^{-i\omega t}=\left(\sum_m a_m\right)\, s(t,\mathbf{0};\hat{\mathbf{u}}_0)\,. \tag{8}$$

In the case that the element amplification factors a_m are all unity, the beamformed signal from direction $\hat{\mathbf{u}}_0$ is just the number of elements times the signal due to the field at coordinate origin, and in general, is intact in shape and is amplified by $\sum a_m$.

We verify that the energy

$$\|z\|^2=\int_{-\infty}^{+\infty}dt\,|z(t)|^2 \tag{9}$$

of the beam-formed signal is maximum when $\hat{\mathbf{u}}=\hat{\mathbf{u}}_0$. As an underlying experimental setup, we are imagining here that the array steering has been fixed to $\hat{\mathbf{u}}_0$, and the direction but not the distance to the point-target is varied, implying that the plane wave packet of Eq. (3) comes from various directions $\hat{\mathbf{u}}$, but is otherwise always the same so that $S_{\hat{\mathbf{u}}}(\omega)=S_{\hat{\mathbf{u}}_0}(\omega)$. We write Eq. (7) in the form

$$z(t,\hat{\mathbf{u}};\hat{\mathbf{u}}_0)=\int d\omega\left\{\sum_m a_m S_{\hat{\mathbf{u}}}(\omega)\mathrm{e}^{i\frac{\omega}{c}[(\hat{\mathbf{u}}-\hat{\mathbf{u}}_0)\cdot\mathbf{R}_m]}\right\}\mathrm{e}^{i\omega t}\equiv\int d\omega Z(\omega)\mathrm{e}^{i\omega t}\,, \tag{10}$$

where

$$Z(\omega)=\sum_m a_m S_{\hat{\mathbf{u}}}(\omega)\mathrm{e}^{i\frac{\omega}{c}(\hat{\mathbf{u}}-\hat{\mathbf{u}}_0)\cdot\mathbf{R}_m} \tag{11}$$

is, in fact, the Fourier-transform of the beam-formed signal. According to Parseval's theorem,

$$\|z\|^2=\int d\omega|Z(\omega)|^2\,. \tag{12}$$

Because, with $a_m\geq 0$ and $S_{\hat{\mathbf{u}}}(\omega)=S_{\hat{\mathbf{u}}_0}(\omega)$, Eq. (11) implies that

$$|Z(\omega)|\leq\sum_m a_m|S_{\hat{\mathbf{u}}}(\omega)|=\left(\sum_m a_m\right)|S_{\hat{\mathbf{u}}}(\omega)|=\left(\sum_m a_m\right)|S_{\hat{\mathbf{u}}_0}(\omega)| \tag{13}$$

it follows from Eq. (12) that

$$\|z(t,\hat{\mathbf{u}};\hat{\mathbf{u}}_0)\|^2\leq\left(\sum_m a_m\right)^2\int d\omega|S_{\hat{\mathbf{u}}_0}(\omega)|^2=\left(\sum_m a_m\right)^2\|s\|^2\,, \tag{14}$$

where $\|s\|^2$ is the energy of $s(t,\mathbf{0};\hat{\mathbf{u}}_0)$. From Eq. (7) and Eq. (14) we see that, indeed, the array gain in the direction $\hat{\mathbf{u}}_0$ is maximal: $\|z(t,\hat{\mathbf{u}};\hat{\mathbf{u}}_0)\|\leq\|z(t,\hat{\mathbf{u}}_0;\hat{\mathbf{u}}_0)\|$.

2.2. Monochromatic signals—time-steering equals phase steering

We will now show that for a monochromatic wave (continuous, not pulsed, sinusoidal wave), time-steering reduces to distortion-free phase steering. Assume that instead of the wave packet of Eq. (3), the wave illuminating the time-steered array is a monochromatic plane wave with angular frequency ω_0 coming coming from direction $\hat{\mathbf{u}}$,

$$s(t, \mathbf{r}; \hat{\mathbf{u}}) = S_0 \mathrm{e}^{i(\frac{\omega_0}{c}\hat{\mathbf{u}}\cdot\mathbf{r} - \omega_0 t)} . \tag{15}$$

This has spectrum $S(\omega) = S_0\delta(\omega - \omega_0)$. Inserting the spectrum to Eq. (7) gives the time-steered beam-former output as

$$z(t, \hat{\mathbf{u}}; \hat{\mathbf{u}}_0) = \sum a_m S_0 \mathrm{e}^{i[\frac{\omega_0}{c}(\hat{\mathbf{u}} - \hat{\mathbf{u}}_0)\cdot\mathbf{R}_m - \omega_0 t]} . \tag{16}$$

We regroup Eq. (16) as

$$z(t, \hat{\mathbf{u}}; \hat{\mathbf{u}}_0) = \sum \left[s(t, \mathbf{R}_m; \hat{\mathbf{u}})\ a_m \mathrm{e}^{-i\Psi_m} \right] , \tag{17}$$

where

$$\Psi_m = \frac{\omega_0}{c}\hat{\mathbf{u}}_0 \cdot \mathbf{R}_m . \tag{18}$$

Equation (17) shows that for a monochromatic wave, the end result of the time-delay-based beam-forming can be also achieved by using the non-delayed signal from each element, but instead applying an element-dependent phase offset Ψ_m across the array. Note incidentally that Eq. (18) shows why we need to take the amplification factors a_m real-valued: if not real-valued, they would directly affect the steering phase.

For the monochromatic wave, phase-steering and time-steering are equivalent, and Eq. (8) therefore says that in the beam maximum direction *neither* method distorts the (now sinusoidal) signal shape. Actually, there is no distortion in any other direction either for the sinusoidal signals, for Eq. (16) says that the beam-formed signal is just the wave's time-form measured at the array origin, multiplied by the array factor AF:

$$z(t, \hat{\mathbf{u}}; \hat{\mathbf{u}}_0) = S_0 \mathrm{e}^{-i\omega_o t} \times \mathrm{AF}(\omega_0, \hat{\mathbf{u}} - \hat{\mathbf{u}}_0) , \tag{19}$$

where

$$\mathrm{AF}(\omega, \mathbf{U}) \equiv \sum_m a_m \mathrm{e}^{i\frac{\omega}{c}\mathbf{U}\cdot\mathbf{R}_m} . \tag{20}$$

2.3. Phase steering

For any incoming wave, monochromatic of not, phase-steering beam-forming is *defined* via Eq. (17) and Eq. (18), by using some representative value for ω_0 in Eq. (18) when computing the element phasing angles.

For the non-monochromatic case, phase-steering has the considerably drawback compared to time-steering that it is dispersive even in the steering direction $\hat{\mathbf{u}}_0$, so that the beam-formed signal cannot be factored as in Eq. (8). Moreover, there is no guarantee that the $\hat{\mathbf{u}}_0$ used in Eq. (18) is really precisely the direction of the maximum gain. In the general case, the phase-steered beam-formed signal for a wave coming from direction $\hat{\mathbf{u}}$ can be written as

$$z = \sum a_m \int d\omega S_{\hat{\mathbf{u}}}(\omega) \mathrm{e}^{i(\frac{\omega}{c}\hat{\mathbf{u}} - \frac{\omega_0}{c}\hat{\mathbf{u}}_0)\cdot\mathbf{R}_m} \mathrm{e}^{-i\omega t} . \tag{21}$$

To proceed, assume that the pulse Eq. (3), though not monochromatic, is strongly band-limited around ω_0, so that we can replace $\omega\mathbf{u}$ in the exponential factor of Eq. (21) by $\omega_0\mathbf{u}$. When that is the case, Eq. (21) factors as the undistorted pulse multiplied by the array factor:

$$z = (\int d\omega S_\omega \mathrm{e}^{-i\omega t}) \times \sum \mathrm{e}^{i\frac{\omega_0}{c}(\hat{\mathbf{u}}-\hat{\mathbf{u}}_0)\cdot\mathbf{R}_m} = s(t,0,\hat{\mathbf{u}}) \times \mathrm{AF}\,. \tag{22}$$

When is it possible to approximate $\omega\mathbf{u}$ by $\omega_0\mathbf{u}$ in Eq. (21)? A sufficient condition is that over the bandwidth of the wave (that is, in the frequency-zone where $S_{\hat{\mathbf{u}}}(\omega)$ is significantly non-zero) the phase angle error

$$\delta\psi = \frac{\omega-\omega_0}{c}\hat{\mathbf{u}}\cdot\mathbf{R}_m$$

caused by the approximation stays small compared to unity, everywhere on the array. Because

$$|\frac{\omega-\omega_0}{c}\hat{\mathbf{u}}\cdot\mathbf{R}_m| \le \frac{2\pi B}{c}L\,, \tag{23}$$

where B is the pulse bandwidth and L is the maximum dimension of the array, we see that a sufficient condition for the most desirable fundamental result Eq. (22) to hold to a good approximation, for all incoming wave directions, is

$$\frac{2\pi B}{c}L \ll 1\,. \tag{24}$$

The bandwidth of a transmitted pulse in reception is a essentially the inverse of the rise time of the pulse, so Eq. (24) says that meaningful phase-steering requires that the time L/c to illuminate the array from end to end must be substantially smaller than the characteristic time $1/B$ for the wave amplitude to change. That is, illumination changes must be "essentially instantaneous" over the whole array. For example, for the planned E3D array with maximum dimension of the order of $L \sim 150$ m, phase steering would be distortion-free only for signal bandwidths that are substantially smaller than 300 kHz. This looks like a good motivation for not to even consider phase-steering for the E3D array; nevertheless, I think it would be of interest to augment GJ's system simulation software to handle phase-steering also, to see just how bad those distortions actually are for typical modulations.

For the rest of this document, and everywhere in the E3ANT package, we will simply assume that the distortions are not so serious as to badly compromise Eq. (22). With that assumption, the array response is the same for all signals, and is given by the array factor AF via Eq. (22). To handle beam forming and beam steering in this approximation, it is therefore neither necessary nor useful to include the signals explicitly.

3. Antenna gain

3.1. Transmission

As a consequence of a regular placement of array elements, the gain pattern of an array may have "grating lobes". That is, there may be are several widely separated "sidelobes" of maximally large gain, so that it appears that the gain pattern has several main lobes. With isotropic elements—the only case we consider in this section—the all the grating

lobes have equal gain in the center of the lobe. The grating lobes are due to maximal constructive interference. In transmission, the interference is between the isotropic, spherical waves emanating from the array elements, so that the the total field $\mathbf{E}^M$ of an M element array in direction $\hat{\mathbf{u}}$ in monocromatic transmission, phase-steered to direction $\hat{\mathbf{u}}_0$, is

$$\mathbf{E}^M(\hat{\mathbf{u}}) = \mathbf{E}_0^M \sum_m \mathrm{e}^{i\frac{\omega}{c}(\hat{\mathbf{u}}-\hat{\mathbf{u}}_0)\cdot\mathbf{R}_m} \equiv \mathbf{E}_0^M \times \mathrm{AF}(\hat{\mathbf{u}}, \hat{\mathbf{u}}_0)\,. \tag{25}$$

$\mathbf{E}_0^M$ is the field due to a single element. The grating directions are by defition those directions where all the exponentials in the AF are equal to unity. Obviously, irrespective of how the array elements are located, at least the direction u_0 is such a direction. It depends on the symmetry of the array if there are other grating directions. In (all) the grating direction(s) $\hat{\mathbf{u}}_g$,

$$\mathbf{E}^M(\hat{\mathbf{u}}_g) = M\mathbf{E}_0^M\,. \tag{26}$$

Array power gain in transmission, $G_T(\hat{\mathbf{u}})$, describes how large the array's field intensity I^M (unit: W/m^2)

$$I^M(\hat{\mathbf{u}}) = \frac{\|\mathbf{E}^M(\hat{\mathbf{u}})\|^2}{\eta}\,, \tag{27}$$

in direction $\hat{\mathbf{u}}$ is compared to the intensity I_0^M of an isotropic radiator of the same total radiated power P^M:

$$G_T(\hat{\mathbf{u}}) \equiv I^M(\hat{\mathbf{u}})/I_0^M\,. \tag{28}$$

All the elements are taken to radiate an equal power P, so that $P^M = M \times P$. If the point of observation of the field is at distance r from the array, we have

$$I_0^M = \frac{P^M}{4\pi r^2} = M\frac{P}{4\pi r^2} = M \times I_0\,, \tag{29}$$

where I_0 is the field intensity we would observe if there would be only a single lone element in the array, radiating with the power P. We denote by $\mathbf{E}_0$ the field of such an isolated radiator, so that

$$I_0 = \frac{\|\mathbf{E}_0\|^2}{\eta}\,. \tag{30}$$

The first puzzlement concerns the transmission gain in the grating directions. What should we expect G_T to be? The field strength is increased M-fold compared to a single radiator, so the field intensity is increased M^2-fold in the denominator of Eq. (28). On the other hand, by Eq. (29), the intensity of isotropic radiation in the nominator of Eq. (28) is increased M-fold. Thus, the gain should have been increased by a factor M compared to the gain (=unity) of a single radiator, so we would expect the grating lobe peak gain to be just

$$G_T(\hat{\mathbf{u}}_g) = M\,. \tag{31}$$

But as Fig. 2–4 shows, even for a two-element array the actual grating lobe gain is not always equal to 2, but varies at least between about 1 and 2.6, depending on the element spacing and the phase-steering angle. Examples later in these notes for larger arrays show that an M-array element has typically gain near M, but not equal to M. How came?

Let's first re-trace the reasoning leading to Eq. (31) to see what the equations Eq. (26)–Eq. (30) *really* imply. We have

$$G_T(\hat{\mathbf{u}}_g) = \frac{I^M}{I_0^M} = \frac{\|ME_0^M\|^2}{M\|E_0\|^2} = M\frac{\|E_0^M\|^2}{\|E_0\|^2}\,. \tag{32}$$

So, if the grating lobe gain differs from the first-order expectation, M, this must be due to the fact that when the M elements are brought together into the array, they no more project precisely the same far field, $\mathbf{E}_0$, as they do when in isolation. Even though they have been forced to radiate the same power in both case. In terms of the equivalent circuitry of a transmitter, Fig. 6, the radiated power of an element is $P = I^2R_r$ where I^2 is the radiation source current and R_r the radiation resistance. The radiations resistance describes how "easily" the antenna is able to convert a driving current to radiation. There does not appear any fundamental reason why that property would *not* depend on array phasing and element spacing. So if R_r changes, and P is forced to be constant (by adjusting the transmitter power amplifier as necessary), I changes. In general, we expect the electric fields generated to be be directly proportional to the source currents, so the changed current would then produce the required change in the projected field.

Referring to the equivalent circuit only serves to confirm that an antenna element can, indeed, accommodate the required field change from the isolated-element situation, without violating any obvious basic principles. But what then is the reason why this field/current change is sometimes required? I think that this is basically due to 3D geometry of the wave interference in transmission. The gain G_T (and hence the field) is determined, both in form and in normalization, when the array factor is given. But the array factor in Eq. (25) is nothing else than a statement that the elementary waves follow the principle of linear superposition when forming the total field. It must be that it is the linear superposition, the formation of the 3D interference pattern, that "forces" the total electromagnetic system to adjust its sources so that the principle can be maintained. Forming the grating lobes involves taking away field energy from some places and placing it in the lobes, in a complicated 3D configuration, and this must be done *without changing the total energy*. The total energy is quadratic in fields, so it does not appear so surprising that the energy zero-sum game does not usually quite succeed with the plain vanilla original fields: there will be some energy left over or some missing when the pattern is formed. To get her sums right, Nature has to enforce an overall adjustment of the single-element field E_0^M. In fact, we do the same adjustment when we compute the array's "power integral", Eq. (59), when computing the absolutely normalized antenna gain.

As a specific example on how the array gain can be different from the simple expectation $G = M$, consider a two-element array where the elements have equal excitation and are located very near to each other compared to the wavelength. In this case, the interference pattern obviously must look much like the field of a single source, that is, nearly isotropic, only with higher intensity. To conserve power, the intensity can now be only twice (not four times) as high as the original single-element intensity. This means that the per-element field must have been reduced from the isolated-element field $\mathbf{E}_0$ to $\mathbf{E}_0/\sqrt{2}$. This requires that the antenna element currents are down by the same factor, $I = I_0/\sqrt{2}$. The radiated power is is I^2R in terms of the radiation resistance R. To conserve power, the radiation resistance must have gone up by a factor of 2, $R = 2R_0$. Note that if we have two such "radiation resistors" side by side, and the

current I goes via both of them, the system looks very much like a single resistor with resistance $1/(1/2R_0 + 1/2R_0) = R_0$ and total current $\sqrt{2}I_0$. This single-element system thus radiates power $2I_0^2R_0$, as required. So the picture is consistent. Of course, the "radiation resistance" is just a way of accounting for the power converted to radiation; the real physical reason for the change of the radiation resistance when the element are brought together must be that the fields produced by one antenna affects the current on the other antennas.

3.2. Reception

Thus, in transmission, the almost-but-not-quite equal-to-M directivity of an array of isotropic elements is a result of an electromagnetic system adjusting itself to energy conservation under the geometric constrains placed on the interference pattern. The basic result concerning antenna gain in reception is that it is equal to the gain of the same antenna used in transmission mode, so, in particular, the gain will be different from M. There is place for confusion here; consider the following reasoning. In reception, it is not at all clear that the argument of the proceeding section can be used to explain how the gain can be different from M. There is only a plane way wave coming in from some direction, and there is no need to adjust a set of elemenrary fields, and hence the element currents, in order to conserver field energy. Moreover, there is an even more serious worry concerning the gain pattern in reception when using off-line beam-forming. (1) Even with element distance fixed, the directivity (in transmission, hence also in reception) depends on the scanning direction. (2) In transmission mode, this required that the elementary currents adjust somewhat. Now assume that we record the element voltages $s_m(t)$ of the array, and then beam-form off-line a whole set of beams by delaying the element signals by various amounts before adding them up to the final beam-formed signal $z(t)$. The different $z(t)$ would then correspond to different beam directions, and hence, different beam directivities. But how can they be associated with different non-M directivities, when there is only a single set element currents?

The confusion is entirely artificial, and is possible because so far we have not really said what we actually mean by "gain in reception", G_R. That crucial thing is, that the *concept*, the physical quantity, gain-in-reception, is not the same quantity than the gain in transmission. Gain-in-transmission describes how the far field of the antenna differs from the field of an isotropic radiator of the same total power, as quantified by Eq. (27). The gain-in-reception relates to entirely different physical situation. It describes how the power received by the array would vary if the same plane way, of fixed intensity, would be be coming from various directions. We can imagine that there is a single point-like transmitter far away, and it is moved on a sphere around the array, always pointing straight towards the array. G_R then quantifies the amount of power received (the voltage squared appearing across the terminals of our array). In fact, to accommodate off-line beam forming, in which case it is not so clear what we mean by "array terminals", we need to be even more careful by what we mean by the array gain.

Finding the grating lobes is a main topic in these notes and will be inspected in detail later, but here we will comment about their "physical significance", especially in the connection of reception. In transmission things appear rather clear-cut. The existence of grating lobes implies that more or less equal amounts of transmission power is directed into multiple widely separated directions. In most cases this is not the wanted behaviour, and so grating lobes in the array's gain pattern must be avoided. This can be

done either by placing the elements near enough to each other; or by using sufficiently directive elements; or by avoiding regular placement of the elements in the first hand. Examples of the gain patterns for a few irregular arrays with isotropic elements are in Fig. 5.

What should one think about the grating lobes in reception? Are they equally disastrous as in transmission? Do the grating lobes even "really exist" in reception? The short answer is that yes, they exist, and yes, they are harmful to some extend. One way to think about the grating lobes, both in reception and in transmission, is to note that

- The grating lobes are nothing else than overly ambitious side lobes.

Therefore, when feeling confused about the meaning of the array grating lobes, compare the situation to the (for the EISCAT community) better-known situation of the side-lobes of the big dish antennas. But as I have never really understood the meaning of the gain pattern in reception, I will attempt to tackle the issue in more detail here. The reader may want to fast-forward to the beginning of section 4.

The main thing to understand about the gain pattern is the mantra that for arrays, just as for dishes, the gain pattern in reception is equal to the gain pattern in transmission. So I will review here how this really comes about, and indeed, what precisely does it mean that the patterns are equal. There is room for confusion here. For instance, it is not difficult to find in the internet statements to the end that transmission and reception gain patterns are equal *because*

1. The Maxwell's equations are time inversion symmetric on one hand, and

2. The fields and currents are closely connected on the other hand,

and *therefore* reception is essentially just the transmission run backward in time.

If this indeed where so, then of course the flows of radiation energy (the antenna pattern) would have same geometry in both cases. But I now think that the above reasoning misses the point. Although both reception (RX) and transmission (TX) do, of course, respect the Maxwell's equation, the boundary conditions of the total system are not anywhere the same in the two situations. In standard TX and RX configurations, the fields, both the driving fields and the total fields, both near the antenna and far away, definitely differ by more than just the sign of time. For TX, we are having some complicated field pattern near the antenna, and a more a less spherical outgoing wave far away. In the standard RX configuration, we are receiving a more a less spherical wave coming from a single well-defined source. I hope that nobody is going to claim that the two basically spherical wave-fields from two widely separated sources only differ by the sign of time! The fact that there are an induced radiation field in RX cannot change this overall field picture. In ideally matched reception a half—but only a half, irrespective of the number and size of the side lobes—of the initially captured wave energy is immediately re-radiated. But that applies to all antennas; nothing special with arrays here. So the bottom line of this paragraph is that the standard RX scheme *is no* the standard TX scheme run backwards in time.

Therefore, I fail to see how the time-reversal invariance can be useful in an argument about the reception gain. More powerful features of electromagnetism are called for to obtain a proof, namely, the principle of reciprocity. That principle, I think—though I'm not really sure—involves more than just the time-reversal symmetry of the Maxwell

equations. But first we need to be careful about what we, actually, want to proof. What are the "standard situations" in RX and TX?

Conceivable, we could imagine really running the transmission backwards, with energy flows coming in from all over the sky. But that would be a very special case, and, would anyone really want to do that, could be handled as a consequence of linear superposition, once we have handled the standard case of a point source first. So, in standard reception situation, we have a small radiation source in direction $\hat{\mathbf{u}}$ as viewed from the receiving antenna.

- The standard concept of "gain in reception" seeks to quantify the variation of the received power, or the size of the induced voltage on the antenna terminals, when the point source's direction but not its distance is varied. Thus, a driving plane wave field's magnitude but not direction in front of the receiving antenna is kept constant, and we want to know how much of the wave's power actually gets in, as function of $\hat{\mathbf{u}}$.

- On the other hand, the standard concept of "gain in transmission" quantifies how much a transmitting antenna's far field intensity, or amplitude, varies as function of direction when the distance to the point of observation is fixed.

There are two different entities involved: (1) the gain-in-transmission and (2) the gain-in-reception. But, fortunately, there are also two different situation to plug these entities in: the TX and the RX situations. Therefore, it is possible, though still miraculous, that the two different gain-quantities can be numerically represented by a single function. This function is then simply called the directional power gain $G(\hat{\mathbf{u}})$ (or the directional amplitude gain $\mathcal{G}(\hat{\mathbf{u}}) = \sqrt{G(\hat{\mathbf{u}})}$, if we want to deal with field amplitudes rather than field intensities). Another point of view is to maintain that there exists only a single gain quantity, namely, the gain in transmission, and the reception directional sensitivity is expressed in terms of the transmission gain.

To proceed this, we need the principle of reciprocity. This is a statement that (under certain conditions) there is a symmetry, reciprocity, in the mutual coupling between subsystems of an electromagnetic system. For a simple electronic two-port circuit, consisting only of linear elements such as shown in Fig. 7, the statement of reciprocity can be phrased in the following way: If a generator current $I_A = I_0$ in port A causes a voltage $U_A^{(B)} = U_0$ in port B, then, if we interchange the current generator and the voltmeter, and again extract I_0 from the generator, the voltmeter again will show the value U_0. For ordinary circuit elements, this result is already built-in into the Kirchoff rules used to compute the internal currents and voltages in the circuit, so that for any given configuration, such as shown in Fig. 7, one may prove the reciprocity by directly computing the voltage U_0 resulting from the driving current I_0.

Although it cannot any more proved from Kirchoff rules, the same reciprocity statement holds also for the two-port system shown in Fig. 8, where subsystem A is the radar antenna of interest, and subsystem B is a small far-away test antenna. From the reciprocity and the linearity properties of the system, we argue in the caption text of Fig. 8 that the directional dependancy of the voltage V_{REC} observed at the terminals of the receiving antenna when the antenna is illuminated with transmission from the test antenna in direction $\hat{\mathbf{u}}$, is solely via $\mathcal{G}_T(\hat{\mathbf{u}})$, where $\mathcal{G}_T(\hat{\mathbf{u}})$ has originally been defined as the gain-in-transmission quantity:

$$V_{\mathrm{REC}} = b \times \mathcal{G}_T(\hat{\mathbf{u}}) \times \|\mathbf{E}_{\mathrm{REC}}\| \,. \tag{33}$$

In Eq. (33), neither b nor $\|\mathbf{E}_{\rm REC}\|$ depend on the direction $\hat{\mathbf{u}}$. The field $\mathbf{E}_{\rm REC}$ is the "driving field", which is just the far field of the test transmitter, and does not contain the re-radiated fields. From the form of Eq. (33) it may appear that a precise definition of the gain-in-reception can be done only up to a normalization constant, for we could as well write the right-hand-side as, say, $(2b) \times (\mathcal{G}_T/2) \times \|\mathbf{E}_{\rm REC}\|$. We could leave this be so, for only the combination $b \times G_T$ is measurable. But we can also fix the normalization by requiring that the gain-in-reception is, well, a gain, that is, integrates to 4π. With this natural normalization, the gain-in-reception becomes precisely equal to the gain-in-transmission, and one may dispense with the subscripts "T" and "R" altogether, as we do in most parts of these notes. Or one can just use G_T even when handling reception, is we do in Eq. (35).

When the normalization is fixed, one can then uniquely determine the constant of proportionality b, by making use of the known radiation field of the test antenna. Instead of computing $V_{\rm REC}$, the normal and more useful way is to compute the actually received power (power delivered to an ideally matched load). This leads to the fundamental expression of the received power in terms of the effective area (effective aperture) $A_{\rm e}$ of an receiving antenna

$$P_{\rm REC} = A_{\rm e} \times \frac{\|\mathbf{E}_{\rm REC}\|^2}{\eta}\,, \tag{34}$$

$$A_{\rm e} = \frac{G_T(\hat{\mathbf{u}})\lambda^2}{4\pi}\,. \tag{35}$$

The flow of logic is that Eq. (34) defines what is meant by the effective area, and then Eq. (35) is the expression found to that quantity by the reciprocity argument. In Eq. (34), η is the impedance of vacuum, 377 Ω, and $\|\mathbf{E}_{\rm REC}\|^2/\eta$, which has the dimension $\mathrm{W/m^2}$, is the intensity of the incoming monochromatic plane wave.

We have re-convinced ourselves that the gain in reception—for any antenna, array or not—is equal to the gain of the same antenna when used in transmission. In EISCAT, we have got accustomed to the idea that even the small side lobes of our dish antennas are a bad thing. By planning now to incorporate array antennas, with their associated huge side lobes (the grating lobes), are we now committing a huge stupidity?

One one hand, it is true that when there are significant side lobes, a significant amount of gain resides in them, and that gain is then not available in the direction of interest, the "main lobe" direction. And that implies loss of signal detection sensitivity. So it may appear that we indeed are doing something wrong.

But on the other hand, it is in the nature of the array that not very much can be done to "move" gain from the non-interesting lobes to the interesting lobes. Naively, if there are N elements, one would expect the maximum gain to be about N times the element gain G_E. Actually, for a regular plain array of reasonably many elements, we show in section 4.10 that the effective area cannot exceed the land area occupied by the elements, and so the maximum gain actually is $N \times 4\pi D^2$ where D^2 is the area occupied by one element in units of λ^2. Thus the maximum gain is limited even more strongly than just by $N \times G_E$ (there appears to be no fundamental limit to how large the gain G_E of an isolated element could in principle be). But as long as G_E is not too large, $G_E < 4\pi D^2$, the gain $N \times G_E$, which is also achieved in practice, is about as large as can be reasonably hoped for.

In summary, for the regular planar array, the sensitivity is almost automatically about as good as can be hoped for, and therefore, any suggestion that we were "losing gain" or

"losing sensitivity" (due) to the multiple grating lobes, is unfair. It is unfair in the same way as it would be unfair to complain that one is losing half of the available receive power to the re-radiation. The re-radiation is unavoidable by the nature of electromagnetism, not because of some incompetent engineering.

What the situation would be if we could allow irregular arrays and non-uniform excitation fields, I don't know. For example, people are talking about "superdirective" arrays : for instance, it is possible to have a linear array of isotropic elements where the gain approaches N^2, but that requires specifically tailored non-uniform spacing and specifically tailored excitation fields.

For conventional array designs, we need not be overly worried about the grating lobes, but that does not mean that we should not be *somewhat* worried about the grating lobes. The situation with arrays is actually not too dissimilar from the situation with dishes. The basic gain pattern, and especially the directivity (maximum gain) of a dish is mainly determined by the geometric aperture, so that only modest improvements in gain can be achieved by tailoring the details. For a sizable conventional planar array, the directivity is also largely determined by the geometric area, and can only be improved by so much by tinkering the details. For arrays, in order to achieve the naturally available directivity, we have the extra degree of freedom that we can use fewer elements if the elements themselves are directive.

There is a prize to that flexibility, or course. The prize is not so much in terms of directivity, (and hence, not in terms of maximum detection sensitivity), but rather in terms of directional aliasing. That is, when the gain in the antenna side lobes (grating lobes or not) is not insignificant, there can be a serious loss of information about the actual target direction. The side lobes can poke all over the sky, and there appears to be no way to determine via which lobe(s) the observed power came in—*unless we know a priori that there is no scattering coming from the non-intesting lobe directions.*

If the large side lobes cannot be suppressed (using directional elements or irregular element placement), we must in the very least arrange things so that potential targets in the side lobes are not illuminated by the transmitter. When the reception antenna is different from the transmission antenna, this should be possible, at least in principle. But how much does this constrain the available pointing schemes in practice, especially when using multi-beam-forming reception, must be inspected carefully.

Another potential penalty for large-gain side lobes is that even if there would be no illumination in the side lobe directions, unwanted external RF signals may easily sneak in. On the other hand, the gain is large in only narrow cones, so perhaps this is not such a serious problem in practice.

4. A phased array

This section introduces the phased-array steering- and gain-related concepts, notations and computations as implemented in the m-files in the E3ANT package.

4.1. The array factor

With reference to Fig. 9, assume that the far-field electric field caused by the antenna element at the origin, in the direction of unit vector $\hat{\mathbf{u}}$, is $\mathbf{E_0}$. Then the far field of the element at position $\mathbf{d_m}$ is $\mathbf{E_m} = \mathbf{E_0}e^{i\Psi_m}$, where Ψ_m is the phase difference of the two waves when they arrive at the target. This difference corresponds to the distance

$\Delta_m = \hat{\mathbf{u}} \cdot \mathbf{d}_m$ of the element from the plane $\mathrm{P_u}$ normal to $\hat{\mathbf{u}}$, and is $\Psi_m = 2\pi\Delta_m/\lambda$. Therefore, the total field at the target is

$$\mathbf{E} = \sum_m \mathbf{E}_m = \mathbf{E}_0 \sum_m \mathrm{e}^{i\mathbf{2}\pi\hat{\mathbf{u}}\cdot\frac{\mathbf{d}_m}{\lambda}} . \tag{36}$$

The sum multiplying the field $\mathbf{E}_0$ in Eq. (36) takes care of the relative phases of the elements caused by their different positions, and is called the array factor AF. There may be also inherent phase and amplitude differences between the elements. These can be accounted for by multiplying the complex exponentials by complex amplitudes b_m, and these can also be bundled into the array factor, which becomes

$$\mathrm{AF}(\hat{\mathbf{u}}) = \sum_m b_m \mathrm{e}^{i\mathbf{2}\pi\hat{\mathbf{u}}\cdot\frac{\mathbf{d}_m}{\lambda}} . \tag{37}$$

The sum goes through all the elements comprising the array.

Often in the litterature the exponent in the array factor Eq. (37) is written in terms of the wave vector $\mathbf{k} = k\hat{\mathbf{u}} = (2\pi/\lambda)\hat{\mathbf{u}}$ of the plane wave arriving to the target from the antenna. In this note, we prefer to work with the dimensionless unit vector $\hat{\mathbf{u}}$ instead, and will write most of our equations in terms of dimensionless quantities only. The basic reason is that the physical problem at hand, the far field antenna gain pattern, depends only on dimensionless quantities, like beam directions and the ratio of various lengths to the wavelength, and is thus inherently dimensionless. We also prefer to work directly on the discrete problem using the tools of discrete math, instead first moving matters to the continuous domain and then returning via Dirac delta-functions. Sometimes, our approach seems to result in slightly more compact equations.[1]

In the e3ant package, we assume that the array is rectangular in shape, regularly spaced, and in the xy-plane, with the longer side along the x-axes. We split the amplitudes $b_m = b_{m_x m_y}$ in such away that we can write the array factor as

$$\mathrm{AF}(u_x, u_y) = \sum_{m_x=0, m_y=0}^{M_x-1, M_y-1} a_{m_x m_y} \mathrm{e}^{i(2\pi u_x D_x - \delta_x)m_x} \mathrm{e}^{i(2\pi u_y D_y - \delta_y)m_y} . \tag{38}$$

Here $D_x = d_x/\lambda$ and $D_y = d_y/\lambda$ specify the array element spacing in the x- and y-directions, and M_x and M_y are the number of element rows in the y-and x-directions. The cartesian x- and y-coordinates u_x and u_y of $\hat{\mathbf{u}}$, also called the direction cosines because $u_x = \cos(\hat{\mathbf{u}}, \mathbf{x})$, uniquely specify the pointing direction in the upper half sphere, the z-component is found by the normalization as $u_z = +\sqrt{1 - u_x^2 - u_y^2}$. The cartesian coordinates can be expressed in terms of the usual spherical coordinates ϕ and θ, where the azimuth angle ϕ is measured in the xy-plane counter-clockwise from the positive x-axis, that is, towards the positive y-axis; and θ is the polar angle, measured from the positive z-axis, and is the complement of the elevation angle. But note that *azimuth* in the EISCAT pointing geometry programs is measured in clockwise direction from the north, irrespective of how our array is oriented. The spherical-to-cartesian conversion is

$$\begin{aligned} u_x &= \sin(\theta)\cos(\phi) \\ u_y &= \sin(\theta)\sin(\phi) . \end{aligned} \tag{39}$$

The standard Matlab function SPH2CART can be used for this transformation.

[1] For instance, compare the equations 9.83-9.86 in Kildal's (factually excellent but typographically horrible) book *Foundations of antennas*, to our Eq. (69).

4.2. Array factor as 2-D discrete Fourier transform of the excitation field

We define a reference direction, $\mathbf{u}_0 = (u_x^0, u_y^0)$, by

$$\begin{aligned} u_x^0 &= \delta_x/(2\pi D_x) \\ u_y^0 &= \delta_y/(2\pi D_y)\,. \end{aligned} \tag{40}$$

The array factor Eq. (38) can then be written more economically using matrix notation as

$$\mathrm{AF}(\mathbf{u}) = \sum_{\mathbf{m}} a_{\mathbf{m}} \mathrm{e}^{i2\pi(\mathbf{u}-\mathbf{u}_0)D\mathbf{m}}\,, \tag{41}$$

where $\mathbf{m} = (m_x, m_y)$, considered a 2×1 column matrix, the row matrix $\mathbf{u} = (u_x, u_y)$, and D is a 2×2 diagonal matrix with D_x and D_y as the elements. We wrote Eq. (41) to resemble as much as possible a two-dimensional analogue of the standard definition of the 1-dimensional Fourier-transform of a sequency of number,

$$\tilde{a}(\nu) = \sum_m a_m \mathrm{e}^{i2\pi\nu m}\,.$$

Indeed, Eq. (41) shows that for the plane array, the array factor AF is simply the 2-dimensional discrete-space Fourier-transform of the two-dimensional sequence $a_{\mathbf{m}}$ of the excitation amplitudes, evaluated at the point $(\mathbf{u} - \mathbf{u}_u)D$:

$$\mathrm{AF}(\mathbf{u}) = \tilde{a}((\mathbf{u} - \mathbf{u}_0)D)\,. \tag{42}$$

4.3. Grating zones and grating directions

The array factor of the regular grid is periodic, just as the the 1-dimensional Fourier-transform is. This periodicity corresponds to kind of directional aliazing: any directions (u_x, u_y) for which (Ψ_x, Ψ_y) differ by $n \cdot 2\pi$ are identical:

$$\mathrm{AF}(u_x + n_x/D_x, u_y + n_y/D_y) = \mathrm{AF}(u_x, u_y), \tag{43}$$

for all n_x, n_y for which the AF argument on left-hand-side stays within the unit circle, also called the circle of visibility in this context, $\{(u_x, u_y) : u_x^2 + u_y^2 <= 1\}$. That means that the visibility circle is divided to size $(1/D_x) \times (1/D_y)$ rectangular cells, over which the AF as a function of (u_x, u_y) repeats periodically from cell to cell. Especially, the maxima of AF are equal, and repeat periodically. The directions $\hat{\mathbf{u}}_g$ of these maxima are called the grating directions of the array.

The cells are analogous to the Nyquist zones in sampled time-signals, and we refer to them either as the Nyquist zones or as the grating zones. It does not matter in a periodic structure where one considers a period to start, but in Fig. 11 we have centered the zones on the grating directions.

4.4. Phase steering

The grating directions depend on the array element spacing D_x and D_y, the parameters δ_x, δ_y, and, if no restrictions are placed on them, also on the complex-valued excitation amplitudes. But it follows from the triangle inequality applied to Eq. (41) that

$$|\mathrm{AF}| \leq \sum |a_{\mathbf{m}}|\,. \tag{44}$$

If we restrict the excitation amplitudes to be real and positive, we can write the right-hand-side of Eq. (44) without the absolute signs. On the other hand, we note from Eq. (41) that the upper limit $\sum a_{\mathbf{m}}$ is reached when $\hat{\mathbf{u}} = \hat{\mathbf{u}}_0$. This means that the reference direction $\mathbf{u}_0$ maximizes |AF|, that is, is one of grating directions. Except when explicitly stated otherwise, we will in these notes restrict the amplitudes to be real and positive. Then the above argument, and the periodicity of AF, show that the grating directions $\mathbf{u}_g$ do not depend on the $a_{\mathbf{m}}$,[2] but can be solved solely from

$$\begin{aligned} \Psi_x &= n_x 2\pi \\ \Psi_y &= n_y 2\pi \end{aligned} \tag{45}$$

or

$$\begin{aligned} 2\pi D_x\, u_x^g - \delta_x &= n_x 2\pi \\ 2\pi D_y\, u_y^g - \delta_y &= n_y 2\pi\,. \end{aligned} \tag{46}$$

We note that the reference direction $\mathbf{u}_0$ corresponds to $n_x = n_y = 0$,

$$\begin{aligned} 2\pi D_x(\, u_x - u_x^0) &= 0 \\ 2\pi D_y(\, u_y - u_y^0) &= 0\,. \end{aligned} \tag{47}$$

When we want to transmit to a given reference direction $\mathbf{u}_0$, the relative phase of the elements, say the initial start-up-phase $\Psi^0_{m_x m_y}$ of the oscillator driving the element (m_x, m_y), must be made to change from element to element across the antenna as

$$\Psi^0_{m_x m_y} = m_x \delta_x + m_y \delta_y, \tag{48}$$

with δ_x and δ_y solved from from Eq. (40) as

$$\begin{aligned} \delta_x &= u_x^0/(2\pi D_x) \\ \delta_y &= u_y^0/(2\pi D_y)\,. \end{aligned} \tag{49}$$

With the definition Eq. (49), δ_x and δ_y will in general not be in the range $[-\pi, \pi]$, nor within any other single interval of length 2π. One might refer to the numbers δ_x and δ_y solved from Eq. (49) as the unwrapped phase steering angles. For plugging into the initial phase $\Psi^0_{m_x m_y}$, δ_x and δ_y can of course wrapped to a fixed interval, say to $[-\pi, \pi]$. In terms of grating directions, we are then just using some other of the equivalent grating directions as the reference direction. For programming, the benefit of using the unwrapped steering angles is that then there is a one-to-one correspondence between the beam direction of interest and the steering angles. Therefore, the unwrapped angels are what are used in this package. Fig. 12 illustrates the use of wrapped and unwrapped steering angles, for an 1-D array with $D_x = 2$.

4.5. The array factor with equal excitation amplitudes

When the excitation amplitudes $a_{m_x m_y}$ are all equal (we take them all equal to unity then), the x-and y-sums in Eq. (38) decouple, and the sum can readily be computed in

[2] This also shows, incidentally, that pure amplitude jitter cannot change the beam maximum direction. In short, we can only have phase-steering, but not "amplitude steering".

closed form as a product of two Direchlet kernels:

$$\begin{aligned} \mathrm{AF} &= \sum_{m_x=0}^{M_x-1} \mathrm{e}^{i\Psi_x m_x} \sum_{m_y=0}^{M_y-1} \mathrm{e}^{i\Psi_y m_y} && (50) \\ &= \mathrm{e}^{i\Phi} M_x M_y \cdot \mathrm{diric}(\Psi_x, M_x) \cdot \mathrm{diric}(\Psi_y, M_y)\,, && (51) \end{aligned}$$

where Φ is a non-observable phase factor, which we ignore,

$$\begin{aligned} \Psi_x &= 2\pi u_x D_x - \delta_x = 2\pi D_x(\, u_x - u_x^0) \\ \Psi_y &= 2\pi u_y D_y - \delta_y = 2\pi D_y(\, u_y - u_y^0) \end{aligned} \qquad (52)$$

and the Dirichlet kernel is defined by

$$\mathrm{diric}(\Psi, M) = \frac{\sin(M\Psi/2)}{M\sin(\Psi/2)}. \qquad (53)$$

The function DIRIC in Matlab signal processing toolbox implements Eq. (53). The magnitude of the Dirichlet kernel is periodic by 2π. One period is plotted in Fig. 10 for a few values of M, using PLOT-DIRIC.M.

4.6. Parseval's theorem

We will need the Parseval's theorem for two-dimensional sequencies. Recall that for the 1-dimensional sequence, Parseval's theorem—spectral domain and power domain representation of signal energy are equal—is

$$\int_0^1 |\tilde{a}(\nu)|^2\, d\nu = \sum_m |a_m|^2. \qquad (54)$$

Moreover, due to $\tilde{a}(\nu)$ periodicity by 1, it follows from Eq. (54) that

$$\int_0^{1/D} |\tilde{a}((\nu-\nu_0)D)|^2\, d\nu = \frac{1}{D}\sum_m |a_m|^2\,, \qquad (55)$$

for any constants ν_0 and D. The 2D-analogue of Eq. (55) holds,

$$\int |\tilde{a}((\mathbf{u}-\mathbf{u}_0)D)|^2\, d^2\mathbf{u} = \frac{1}{D_x D_y}\sum_{\mathbf{m}} |a_{\mathbf{m}}|^2\,. \qquad (56)$$

4.7. Antenna gain and the power integral

The directive gain (which we will also call power gain in this note) of an antenna in the direction $\hat{\mathbf{u}}$ is the ratio of the power radiated per unit solid angle into that direction, divided by the power density of the same total power radiated isotropically,

$$G(\hat{\mathbf{u}}) = \frac{dP}{d\Omega} \Big/ \frac{P}{4\pi}\,. \qquad (57)$$

The power density is proportional to the squared modulus of the total field, so is proportional to $|\mathrm{AF}|^2$. If the antenna elements themselves have non-isotropic gain, all equal to $G_\mathrm{E}(\hat{\mathbf{u}})$, the power density $dP/d\Omega$ is proportional to $G_\mathrm{E}(\hat{\mathbf{u}})\mathrm{AF}(\hat{\mathbf{u}})^2$,

$$G = \frac{1}{\mathrm{PI}} \cdot G_\mathrm{E}\, |\mathrm{AF}|^2. \qquad (58)$$

From Eq. (57) we Eq. (58) we get antenna's "power integral" PI as

$$\mathrm{PI} = \frac{1}{4\pi} \int_{4\pi} G_{\mathrm{E}} \, |\mathrm{AF}|^2 \, d\Omega \, . \tag{59}$$

The array factor can always be evaluated numerically directly from the defining sum Eq. (41); or by computing the 2D Fourier transform Eq. (42) by FFT; or, as we mostly do in this package, where we take the excitation field as constant, even from the closed expression Eq. (50). For many purposes, like when inspecting pointing accuracy, this is already enough, for only the relative gain, that is, the gain relative to the maximum level, the beam center, may be of interest. But when the attainable signal levels are of concern, the absolutely normalized gain of Eq. (58) is required. The problem then is to evaluate the power integral.

4.8. The power integral for an array with isotropic elements

For the array with isotropic elements, $G_{\mathrm{E}} = 1$, the power integral over the full solid angle can readily be evaluated. The squared magnitude of the array factor is

$$|\mathrm{AF}|^2 = \sum a_{\mathbf{m}} \overline{a}_{\mathbf{m}'} \mathrm{e}^{i2\pi \mathbf{u}_0 D(\mathbf{m}-\mathbf{m}')} \mathrm{e}^{i2\pi \mathbf{u} D(\mathbf{m}-\mathbf{m}')} \tag{60}$$

The only non-trivial step is to evaluate the integral

$$I = \int_{4\pi} \mathrm{e}^{i2\pi \mathbf{u} D(\mathbf{m}-\mathbf{m}')} \, d\Omega(\hat{\mathbf{u}}), \tag{61}$$

Noting that the orientation of the coordinate system does not matter when integrating over the full solid angle, we will orient the z-axis of our 3D spherical coordinate system along the direction of the vector $D(\mathbf{m} - \mathbf{m}')$, so that θ is the polar angle of $\hat{\mathbf{u}} = (\mathbf{u}, u_z)$ from that direction, and hence the integrand in I becomes

$$\mathrm{e}^{i2\pi \cos\theta \|D(\mathbf{m}-\mathbf{m}')\|} \sin\theta d\theta d\phi \, .$$

The integral can be immediately evaluated over θ (and trivially,ϕ), to give

$$I = 4\pi \, \mathrm{sinc}(2\pi \|D(\mathbf{m} - \mathbf{m}')\|) \, . \tag{62}$$

The power integral thus is

$$\mathrm{PI} = \sum \mathrm{a}_{\mathbf{m}} \overline{\mathrm{a}}_{\mathbf{m}'} \, \mathrm{sinc}(2\pi \|\mathrm{D}(\mathbf{m} - \mathbf{m}')\|) \, \mathrm{e}^{\mathrm{i}2\pi \mathrm{u}_0 \mathrm{D}(\mathrm{m}-\mathrm{m}')} \, . \tag{63}$$

It may be observed that $G = |\mathrm{AF}|^2/\mathrm{PI}$, with AF taken from Eq. (60) and PI from Eq. (63), has the expected special cases. For instance, when $D_x = 0$ and $D_y = 0$, we have only one, isotropic, element, so we expect $G \to 1$ when $D_x \to 0, D_x \to 0$, and this clearly happens. For the case of two elements along the x-axis, $a_{00} = 1$ and $a_{01} = \pm 1$, with $D_x = D, D_y = 0$, the absolutely normalized gain is

$$G = \frac{1 \pm \cos[2\pi D(u_x - u_x^0)]}{1 \pm \mathrm{sinc}(2\pi D) \cdot \cos 2\pi D u_x^0} \, , \tag{64}$$

where $u_x = \sin\theta$, $u_x^0 = \sin\theta_0$. Here, as in general, the normalization depends both on the array spacing, the excitation pattern, and the beam direction.

4.9. The power integral for an array with directional elements

When the element gain $G_{\rm E}$ depends on direction, the power integral cannot in general evaluated in a closed form. However, for arrays with reasonably large number of elements both in the x- and y-directions, an approximation can be found as follows. For such an array, the array factor resembles a sum of delta functions, that is, AF has narrow beams around the widely separated grating directions, and pretty much zero elsewhere. Denoting by $\Delta\Omega_g$ the solid angle around the grating direction $\mathbf{u}_g$ that contain the essential part of the AF in that direction, we write the power integral as the sum of integrals over the support regions,

$$4\pi \cdot \mathrm{PI} = \int_{4\pi} G_{\rm E}\,|\mathrm{AF}|^2\,d\Omega \approx \sum_g \int_{\Delta\Omega_g} G_{\rm E}|\mathrm{AF}|^2\,d\Omega\,. \tag{65}$$

We assume that the element gain is wide compared to the size $\Delta\Omega_g$, so that we can take $G_{\rm E}$ to be constant in that region, and take it out of the integral, and use Eq. (42) to replace AF by the 2-D Fourier transform of the excitation amplitude-sequence,

$$4\pi \cdot \mathrm{PI} \approx \sum_g G_{\rm E}(\mathbf{u}_g) \int_{\Delta\Omega_g} |\tilde{a}((\mathbf{u}-\mathbf{u}_0)D)|^2\,d\Omega(\hat{\mathbf{u}})\,. \tag{66}$$

The differential surface element, on the surface of unit sphere, corresponding the solid angle $d\Omega$, is equal of the size of the projection $d^2\mathbf{u}$ to xy-plane of that surface element, divided by the cosine of the polar angle θ_g of $\hat{\mathbf{u}}$ at the element,

$$dS_g(\hat{\mathbf{u}}) = \frac{d^2\mathbf{u}}{\cos\theta_g}\,. \tag{67}$$

This corresponds to change of variables from the spherical coordinates on the surface of the sphere to the cartesian coordinates on the xy-plane. The precise boundary of the area of integration does not matter, as it anyway is assumed to be in the 0-region of the integrand. We make the substitution Eq. (67) to Eq. (66). Then we also expand the area of integration to cover the whole grating zone Z_g hosting the direction $\mathbf{u}_g$; this just adds some more 0-region to the area, for there is at most one grating beam in a grating zone. The power integral becomes

$$4\pi \cdot \mathrm{PI} = \sum_g \frac{G_{\rm E}(\mathbf{u}_g)}{\cos\theta_g} \int_{Z_g} |\tilde{a}((\mathbf{u}-\mathbf{u}_0)D)|^2\,d^2\mathbf{u}\,. \tag{68}$$

Finally, we use Parseval's theorem for 2-D sequencies, Eq. (56), to get

$$\mathrm{PI} = \left(\sum_g \frac{G_{\rm E}(\mathbf{u}_g)}{\cos\theta_g}\right) \frac{1}{D_x D_y} \frac{\sum |a_{\mathbf{m}}|^2}{4\pi}\,. \tag{69}$$

4.10. Array gain for an array with directional elements

Consider an array with the excitation amplitudes all unity, and directional elements with power gain $G_{\rm E}$. From Eq. (50), Eq. (58) and Eq. (69), the absolutely normalized gain is

$$\begin{aligned} G(\hat{\mathbf{u}}) &= \frac{G_{\rm E}(\hat{\mathbf{u}})(M_x M_y)^2[\mathrm{diric}()\mathrm{diric}()]^2\;4\pi D_x D_y}{M_x M_y \sum_g \frac{G_{\rm E}(\mathbf{u}_g)}{\cos\theta_g}} \\ &= \frac{G_{\rm E}(\hat{\mathbf{u}})}{\sum_g \frac{G_{\rm E}(\mathbf{u}_g)}{\cos\theta_g}} \frac{4\pi A}{\lambda^2} \cdot [\mathrm{diric}()\mathrm{diric}()]^2\,, \end{aligned} \tag{70}$$

where we used

$$D_x D_y M_x M_y = \frac{d_x M_x d_y M_y}{\lambda^2} = \frac{L_x L_y}{\lambda^2} = \frac{A}{\lambda^2}\,.$$

The factor diric()diric() is unity in the grating directions, so the maximum gain, the antenna directivity $\mathcal{D}(\hat{\mathbf{u}})$, to grating direction $\hat{\mathbf{u}}$, is

$$\mathcal{D}(\hat{\mathbf{u}}) = \frac{g_{\mathrm{E}}(\hat{\mathbf{u}})}{\sum_g \frac{g_{\mathrm{E}}(\mathbf{u}_g)}{\cos\theta_g}} \frac{4\pi A}{\lambda^2}\,. \tag{71}$$

The grating sum $\sum_g$ is to be evaluated over all the grating directions $\mathbf{u}_g$ which are the periodic replicas of the given direction $\mathbf{u}$, in the visibility circle, by period $1/D_x$ in x-direction and $1/D_y$ in y-direction.

If $D_x < 0.5$ and $D_y < 0.5$, the grating sum contains only the single element $\mathbf{u}_g = \mathbf{u}$. For such a dense array, the directivity depends on the beam direction,

$$\mathcal{D}(\hat{\mathbf{u}}) = \frac{4\pi A \cos(\theta)}{\lambda^2}\,, \tag{72}$$

but does not depend at all on the element pattern, nor the element spacing (as long as it is denser than the above limit). For instance, if the area of our benchmark 50×20 array of density $D = 1.5$ wavelength, would be covered with 0.5 wavelength spacing or tighter, the broadside ($\theta = 0$) gain would always be $4\pi \times 50 \times 20 \times 1.5^2 = 44.5$ dBi. The result is geometrically natural, as it says that the effective area $A_{\mathrm{eff}} = G\lambda^2/4\pi$ of the antenna is just the area of the antenna as seen from the target, that is, is equal to the projection of the area to the direction perpendicular the beam direction. Interestingly, the result is analogous to the sampling theorem result for time-signals, which says that if the signal is sampled fast enough, namely, so fast that there can be no aliazing, then no information is lost. In the dense array case, what seems to happen is that when the incoming plane way is sampled tightly enough in space—so tightly that no directional aliasing can occurs—again "no signal is lost", now in the sense that the element grid behaves as it would cover without holes all of the area that is within its outer boundaries. We cannot perhaps hope to do any better, and that might be why the element gain does not effect the overall gain at all.

For less dense grids, the elements (non-normalized) gain, g_{E}, affects the array beam shape and directivity.

4.11. Gain model for the array element

We will assume a simple analytical form for the array element gain. We will assume circular polarization, and will assume axially symmetric element power gain pattern. As suggested by Kildar (p. 61), we will use the form

$$G_{\mathrm{E}} = G_{\mathrm{E}}(\theta') = G_{\mathrm{e}} \cos^{n_e}(\theta'/2)\,, \tag{73}$$

where θ' is the angular offset from the axis direction (ϕ_E, θ_E) of the element. Normalization of G_{E} to 4π over the solid angle gives the relation

$$n_e = 2\,G_e - 2 \tag{74}$$

between the pattern exponent n_e and the maximum gain G_e. The relation between G_e and the half-power beam width W_e follows from $0.5 = [\cos(W_e/4)]^{2G_e-2}$,

$$W_e = 4 \arccos[0.5^{1/(2G_e-2)}] \quad (75)$$

$$G_e = 0.5 \left(2 + \frac{\log(0.5)}{\log[\cos(W_e/4)]}\right) . \quad (76)$$

For instance, for a 10 dBi element, $G_e = 10$, and Eq. (75) gives beamwidth $W_e = 63°$. The gain pattern of this element, as well as the element which has width 40°and gain 13.7, are shown in Fig. 13.

4.12. Computing the antenna directivity and beamwidth

The function POWERINT computes the arrays's power integral from Eq. (69) and the directivity from Eq. (71), for the case of unit excitation amplitudes. Function PLOT_DIRECTIVITY can be used to plot the directivity as a function of the beam direction. The curve is generated by tracking the maximum gain of a given beam when it is phase-steered; that beam is not necessarily the strongest beam of the array at all steerings.Figure 19 shows the directivity of an 50×20 array with 1.5 wavelength spacing, assuming an element with 10 dBi gain, both when the element is pointed in the array broadside direction, and when the element has been tilted 40° from the vertical. The directivity of a dense array of the same physical size is also plotted for comparison, from Eq. (72).

To find antenna beam width, having the non-normalized gain $g_{\mathrm{E}}|\mathrm{AF}|^2$ is sufficient. In fact, the element pattern is normally so wide compared to the grating beams of AF that we can compute the antenna beamwidth from the array factor alone. Function BEAMWIDTH computes the beamwidth in a vertical (fixed ϕ) plane, basically by solving numerically the equation

$$\mathrm{AF}(\theta, \phi_0) = 1/\sqrt{2} \quad (77)$$

in the neighbourhood of the beam direction (ϕ_0, θ_0). The explicit diric()diric() form ,Eq. (50), is used for the AF.

Even though BEAMWIDTH does not resort to the shortcut, it would be sufficient to solve numerically only the beamwidth of a vertical beam, since the vertical beamwidth as a function of the polar angle in a given ϕ plane scales very precisely as $1/\cos\theta$. To see this, note that in a fixed vertical plane, AF is a function of $u_x - u_x^0$, that is, $\mathrm{AF} = f(\sin\theta - \sin\theta_0)$, for some function f. Linearizing the argument of f in the neightbourhood of θ_0 as $(\cos\theta_0)(\theta - \theta_0)$, we can state the equation Eq. (77) for the beamwidth W as

$$f[\cos\theta_0 \cdot (W/2)] \approx 1/\sqrt{2} .$$

The right-hand-side is a constant, so the product $\cos\theta_0 \cdot (W/2)$ must also be approximately constant when θ_0 is varied.

The function PLOT_MAXGAIN is an expanded version of PLOT_DIRECTIVITY, and plots into a single figure both the directivity, the vertical beamwidth, and the element's gain, as a function of polar angle; an example is shown in Fig. 14. The element gain has been normalized to unity at the maximum, and the antenna directivity has been normalized by dividing with the "reference gain" G_{ref}, which we define to be the elements directivity (element's maximum absolutely normalized gain G_{e}) multiplied by the number of elements in the array,

$$G_{\mathrm{ref}} = M_x M_y \mathcal{D}_{\mathrm{E}} . \quad (78)$$

The benefit of the reference gain is that it is an invariant measure of gain for a given array.[3] In particular, it does not depend on the phase steering. And at the same time, is a rather good approximation of the maximum directivity. In many plots we express the gain relative to $G_{\rm ref}$. For the 1000 element array of 10 dBi elements, the reference gain is 10000, or 40 dB. It can be seen in Fig. 14 that with these normalizations, the antenna gain, indeed, follows "on the average" the element's gain pattern.

In Fig. 19 it can be noted that the directivity curve is very smooth when the elements have been directed vertically, but has deep downwards spikes when the elements have been tilted by 40°. To understand why, it us useful to have a global view of the grating directions and their relation to the element gain pattern and the circle of visibility. Such a view is provided by the function PLANEARRAY, which we describe next.

4.13. Array gain and grating directions

The function PLANEARRAY plots in one panel the array's array factor and element gain pattern in arbitrary vertical planes as function of the polar angle (by default, the plotting plane is determined by the element's direction). A separate panel shows a a zoomed-in part around the maximum value (in the chosen plane) of the relative gain $(1/G_{\rm ref})G_{\rm E}|{\rm AF}|^2$. And there is a third panel that shows the grating directions in the u_xu_y-plane, the circle of visibility, and the projection of the antenna elements halfpower cone to the u_xu_y-plane. An example is Fig. 16. If allowed by a flag, PLANEARRAY draws into a separate window a 3-D version of the grating-direction panel of the main figure. This can then be freely rotated interactively on screen using Matlab's built-in interaction tools. An example is Fig. 17.

One of the uses of PLANEARRAY is in trying to understand the behaviour of results produced with more specialized functions of the package. For example, in Fig. 20 we have used PLANEARRAY to find out the rationale behind the dips in the directivity curves that sometimes are there, and sometimes not.

There is considerable amount of (slightly redundant) information packed into the header of the PLANEARRAY output figure Fig. 16.

ARRAY This line gives the array size as number of columns (M_x) and number of rows (M_y), the element spacing in the x- and y-directions (D_x, D_y) in units of wavelength, and the unwrapped phase-steering angles δ_x and δ_y for the marker beam, which is beam 1 in the figure's Grating Panel. The steering angles relate via Eq. (40) and Eq. (39) to the direction ϕ, θ of the marker beam, given in header line 3. In the input section of PLANEARRAY.M, the phase steering can be specified either directly in terms of δ_x and δ_y, or via the required direction of the marker beam.

ELEMENT This line specifies the direction of the array element (ϕ, θ), the half power beam width (w), and the directivity (G). The element is assumed to be of the simple form $\cos^n(\theta/2)$ as described in section 4.11. The last item ($A_{\rm eff}/A$), the ratio of effective area to the physical area, is computed for the current phase steering, and corresponds to the maximum directivity among the grating beams, which may

[3] Another possibility would be to use as the gain reference the maximum directivity of a similarly sized dense array. $G_{\rm ref}$ is a little easier to calculate, and also seems to be numerically more near the maximum directivity for our typical non-dense arrays.

or may not be the directivity of the marker beam. The ratio is computed as

$$A_{\text{eff}}/A = \frac{\max_g \mathcal{D}_g}{4\pi M_x M_y D_x D_y} \,. \tag{79}$$

BEAM 1 This line gives the direction of the marker beam, (the beam 1, marked as the blue solid dot in the Grating Panel), the vertical half-power width (w) of the marker beam as computed by BEAMWIDTH, the directivity of the marker beam ($\mathcal{D}_1$) and the next stongest beam ($\mathcal{D}_5$) (if the beam 1 is not the strongest beam, the directivity of the strongest beam is given), and the reference gain (G_{ref}). The directivities are given with respect to the reference gain, which is computed from Eq. (78). The directivities are found by computing the absolutely normalized gain in the grating directions using Eq. (71).

GRATING This line lists the directions and directivities of all the grating beams, starting with the marker beam. The directivities are given with respect to the reference gain.

4.14. 2-D beam cross section

The vertical beamwidth for a few array sizes is plotted in Fig. 15, when the beam is in the xz-plane. However, the width of the beam in a fixed vertical plane is not a a complete measure of the beam size. To get a complete picture, it is desirable to plot the gain in the whole plane of the beam cross section, for instance, as gain-countor plot. The relative gain

$$g(\phi, \theta) = g_{\text{E}} |\text{AF}|^2 \tag{80}$$

if sufficient for this purpose. Function ARRAYGAIN evaluates Eq. (80) in arbitrary directions for the regularly spaced xy-array, using the analytic diric()diric() form for the array factor, and assuming the simple $\cos^{(}\theta/2)$ form for the array element. The function BEAMSHAPE2D uses ARRAYGAIN to compute and plot the beam cross sections. Only the array factor AF is actually included into the gain computation, though, which means that the beam side-lobes will be somewhat inaccurate. The gain is normalized to unity at the beam center.

A few examples are in Fig. 18. The cross section is expressed in proper angular units, by dividing ϕ by the sine of the polar angle. The plots show the 0.5, 0.1 and 0.01 relative power contours. Only the last one is visible in any of the side lobes. The vertical beam width, computed separately by BEAMWIDTH, is also indicated in the plots. The present implementation of BEAMSHAPE2D cannot handle vertical or near-vertical pointing. Also, the computation takes a noticeable amount of time, about 15 seconds on a 2 GHz G5, when using a 300×300 grid. (One should perhaps try the 2-D FFT method here, perhaps it would be faster, even though we would need quite long FFTs to get comparable angular resolution.)

5. Phase and time accuracy

How accurately does one need to be able to control the phase-steering element-to-element phase steps δ_x and δ_x? If δ is changed systematically by $\Delta\delta$, the beam direction θ changes by an amount $\Delta\theta$, which is calculable from Eq. (40) and Eq. (39). But because

also the array beam width depends on the pointing direction, it is not quite obvious how "pointing accuracy" or pointing granularity should be usefully defined. Namely, if the beam is wider, there is less need to have its direction exactly along some nominal direction. The same applies to the desirable pointing granularity: there is not much sense to change the nominal beam direction at all if the change is only a very small part of the beam width. Therefore,

- It seems appropriate to normalize the directional error tolerances and the granularity requirements by the beam width.

Due to the $1/\cos\theta$ factor, we would be more tolerant against $\Delta\theta$, and require less θ-granularity, in low elevations than on high elevations.

What implications would accepting such a θ-dependent approach have to the phase/-time accuracy requirements? We will argue below that the implications would be all for the good.

While the relation between an applied phasing step δ and the resulting beam direction θ is non-linear[4] the relation between δ and the $u-$ or Ψ-variables is linear; that is, δ is pretty much the same as u or Ψ. Anything that is simple in terms of u, will also be simple in terms of δ. And one of the simple things will be the normalized quantities. To verify this, note that the beam's width in the u-space, W_u, will be the same number W_u everywhere in the u-space, because beam steering just shifts the grating zones as a whole, without "deforming" them. This in turn follows already from Eq. (41), which shows that the array factor depends only on the *difference* $u - u_0$. Thus, if du is some tolerance, or a granularity cell dimension in the u-space, the ratio du/W_u will be constant in the u-space. For *small* du and W_u, a constant ratio du/W_u will imply the same, constant, ratio in terms of *any* variable, such as the θ, that depends smoothly on u. This confirms that the normalized quantities of type $d\theta/W_\theta$ will not depend on the pointing direction, and are therefore the natural ones to specify and describe tolerances and granularities.

We want the quantitative relation between chances of δ_x and δ_y, and chances in the normalized quantities. In terms of the phase variable $\Psi_x = 2\pi u_x D_x$, the effect of phase steering by δ_x is to translate the array factor $\mathrm{AF}(\Psi_x)$ by δ_x, without changing its shape. The change $\Delta\delta$ shifts the pattern $\mathrm{AF}(\Psi)$ by $\Delta\Psi = \Delta\delta$, and changes the beam direction by $\Delta\theta$. What is the relation between $\Delta\delta$ and the normalized change $\Delta\theta/W_\theta$?

It suffices to study $\mathrm{AF}(\Psi)$ around the origin. In terms of Ψ, the array's half power beamwidth corresponds to the Ψ-interval $w_\Psi = 2\Psi_+$, where

$$\frac{1}{\sqrt{2}} = \mathrm{diric}(\Psi_+, M) \approx \frac{\sin(\Psi_+ M/2)}{\Psi_+ M/2}\,. \tag{81}$$

We solve this to get $\Psi_+ M/2 = 1.3916$, so that

$$w_\Psi = \frac{5.57}{M}\,. \tag{82}$$

Because

$$\frac{\Delta\Psi}{w_\Psi} \approx \frac{\Delta\theta}{W_\theta}\,, \tag{83}$$

we get

$$\Delta\delta = \Delta\Psi = \frac{\Delta\Psi}{w_\Psi} w_\Psi \approx \frac{\Delta\theta}{W_\theta} \cdot \frac{5.57}{M}\,. \tag{84}$$

[4] Basically, the relation is via the same $1/\cos\theta$ factor as the relation between beam tilt and beam width. When using normalized quantities, the $1/\cos\theta$ factor cancels out.

For instance, δ_x granularity $\Delta\delta_x = \Delta\Psi_x = 5.57/M_x$ corresponds to beam-width sized granularity, for all elevations. The above argument applies to the y-direction also. So the grid of uniform, beam-with adjusted beam-steering steps is just a regularly spaced grid of (δ_x, δ_y) -values. To get the full half-sphere of directions, it is sufficient and necessary to have one grating zone covered by such a grid. For instance, for a 50×20 array, a "$0.1\times$ beamwidth" granularity-spec would require about $2\pi 2\pi/(0.1 \times 5.57/50)(0.1 \times 5.57/20) = 127000$ distinct directions.

5.1. Timing accuracy versus pointing accuracy

Conceptually, to phase an array with the phasing steps δ_x and δ_y, one would compute an initial phase offset matrix

$$\delta(m_x, m_y) = m_x\delta_x + m_y\delta_y \tag{85}$$

and load the phase offset registers of the DDS system at each element (m_x, m_y) with these values, and clear the phase accumulators to zero. Then all the DDSs would start generating an output phase at a common moment of time, at the desired radar RF frequency f_{RF}. The phase offset register would have enough bits to divide 2π down to milliradians, so to get accurate initial offsets into the offset-registers should not be a problem. But we will assume in this model for the phase jitter that the exact moment of the DDS start varies a little from element to element. We will assume that the start time error is a gaussian random variable with zero mean and standard deviation Δt.

In this model, the phase of transmission at element $n = (m_x, m_y)$ would be

$$\Phi_n(t) = 2\pi f_{\mathrm{RF}}(t + dt_n) + \delta(n) = [2\pi f_{\mathrm{RF}} t + \delta_n] + 2\pi f_{\mathrm{RF}} dt_n\,, \tag{86}$$

where dt_n is the random error in the DDS start time and δ_n is the programmed phase. This means that there is a random error in the relative phases of the elements which also has zero mean, and standard deviation

$$\Delta\psi = 2\pi f_{\mathrm{RF}}\Delta t\,. \tag{87}$$

With f_{RF}= 225 MHz, the numeric relation is

$$\Delta\psi\ [^\circ] = 8.1 \times 10^{-2}\Delta t\ [\mathrm{ps}]\,. \tag{88}$$

Beam-with-sized pointing granularity for a $M = 50$ array requires phasing step 6.4°. If we insert 6.4° to Eq. (88), we get $\Delta t = 79$ ps, which looks like a short time. And, worse, we will need to point the arrays with clearly better than a beam-width granularity, perhaps with a $0.1\times$beam-with granularity. Does this mean that we are in a trouble? No, we no not need to control element timing with 8 ps accuracy. To be able to point the array with $0.1 \times W_\theta$ accuracy on a $M = 50$ array, we would need "only" to be able to

1. Set the phase offset at each elements with 0.64°resolution (10 bits), and
2. Start the DDSs without having a timing error *gradient* across the array.

A constant offset clearly would not matter, and we will show below by simulation that small random offsets do not matter (much), either. What would change the pointing

direction would be if the start time error would *vary systematically* across the array, say increase with a constant step from element to element.

It is possible to imagine the DDS start timing to be implemented in such a way that systematic start time gradient would occur naturally. For instance, if we were using a trigger that spreads from the origin across the array. Or if we were having a part DDS, part analog up-conversion to RF, the analog LOs, even though obviously being phase-locked, could still have a systematically increasing initial phase across the array. To be avoided.

Instead, all the DDSs should (conceptually) have their own clock, which starts the DDS using only information that is independent of the pointing direction. Say, starts after a hardwired, calibrated-once, element-depending, delay after receiving a centrally generated trigger pulse. Or starts directly based on some pre-programmed instant of time at the element's local clock.

Even small random timing errors will to some degree resemble an overall phasing gradient, and thus change the beam direction. And even if not changing the beam direction, the timing jitter would cause incoherence to the array's radiation, and this would reduce the available level of constructive interference that is the basic of the beam-forming, and thus would reduce the maximum available gain. Simulation seems to indicate that the actual required timing accuracy is not anywhere near the 8 ps. Rather, it appears that someting like 100 ps would already be enough.

6. Jitter calculations

6.1. Method

To allow both amplitude and phase jitter at the antenna elements, we write the array factor as

$$\mathrm{AF}(u_x, u_y) = |\sum_{m_x}\sum_{m_y} a_{m_x m_y} \mathrm{e}^{i\psi_{m_x m_y}} \mathrm{e}^{i2\pi D_x (u_x - u_x^0) m_x} \mathrm{e}^{i2\pi D_y (u_y - u_y^0) m_y}|\,, \tag{89}$$

where $u_x^0 = \delta_x / 2\pi D_x$ and $u_y^0 = \delta_y / 2\pi D_y$ are the direction cosines of the phase-steered beam. The amplitudes a are taken to jitter around unity with a distribution that we will take to normal with variance Δa

$$a = 1 + \mathrm{N}(0, \Delta a). \tag{90}$$

The errors ψ of the steering phase steps δ_x and δ_y will be normally distributed around zeros with standard deviation $\Delta\psi$

$$\psi = \mathrm{N}(0, \Delta\psi). \tag{91}$$

Without any jitter, the maximum value of AF, the (relative) gain in direction (u_x^0, u_y^0), is equal to the number $N = M_x M_y$ of array elements. The first observation is that, with only phase errors, but not amplitude errors,

$$\mathrm{AF}(u_x, u_y) <= \sum_n |\ldots| = N,$$

and there can be equality only if all the phases ψ_n are zero. The power integral, Eq. (69), normalizing the gain should not depend much on small changes of the phases of the

excitation amplitudes, so the phase errors will mean that the maximum gain gets lower. Changes of the magnitudes of the excitation amplitudes would cause first-order changes in the power integral which contain the factor $\sum |a_n|^2$. We avoid this by constraining the sum always to be equal to N in the simulation.

We will only consider pointing and beam shape in the $\phi = 0$ plane, and will assume that the phase-steered pointing also is in this plane so that $\phi_0 = 0$, too. Then the last exponential factor in Eq. (89) is always unity, and the array factor in direction θ_k becomes

$$\mathrm{AF}(\theta_k) = \Big| \sum_{m=0}^{M_x-1} \left(\sum_{n=0}^{M_y-1} a_{m,n} \mathrm{e}^{i\psi_{m,n}} \right) \mathrm{e}^{i\Psi_k m} \Big| \,, \tag{92}$$

where $\Psi_k = 2\pi D_x(\sin\theta_k - \sin\theta^0)$.

The simulations are done by the function PLANEARRAY_JITTER. A simulation run consists of a number of trials, and has the following six steps.

1. As input, specify element's timing jitter Δt in picoseconds and element's amplitude jitter Δa around the value 1. Specify the direction of the undistorted beam θ^0. Specify the number of trials. Specify the number of points in the θ_k-grid.

2. From the timing jitter standard deviation Δt, compute the corresponding phase jitter $\Delta\psi$.

3. Select the range for θ_k so that it covers the expected main beam around the given θ^0, and a few side maxima around it.

4. Compute the fiddle-factor matrix $Z(m,k) = \mathrm{e}^{\Psi_k m}$. This is common to all trials of the run and needs to be computed only once.

5. In each trial

   a) Use the random number generator RANDN to generate the matrices $(a_{m,n})$ and $(\psi_{m,n})$, having the distributions Eq. (90) and Eq. (91).

   b) Normalize the amplitudes by dividing each of them by $\sum_{m,n}(a_{m,n})^2 = 1$.

   c) Compute $\mathrm{AF}(\theta_k)$ by direct summation according to Eq. (92).

   d) Estimate beam maximum direction, gain, and halfpower beamwidth by inspecting $\mathrm{AF}(\theta)$, and append these three numbers to the three vectors of results.

6. Using the result vectors, produce a result plot, such as Fig. 21. The plot shows the distribution of the amplitude change, the beam direction change, and the beam width change in the simulation run, as

   a) Histogram of the beam amplitude change away from the expected value 1,

   $$\Delta|\mathrm{AF}| = |\mathrm{AF}|_{\mathrm{trial}} - 1.0 \,.$$

   Note that this is the array factor magnitude change. Change of the gain $G = |\mathrm{AF}|^2$ is about twice as large in the %-units used in the histogram. The mean value and standard deviation of $\Delta|\mathrm{AF}|$ over the trials is shown as item one in line three of the plot header.

b) Histogram of the beam direction change around the value θ^0

$$\Delta\theta = \theta^0_{\text{trial}} - \theta^0 \,.$$

The mean value and standard deviation of $\Delta\theta$ over the trials is shown in line three of the plot header.

c) Histogram of the beam width change from the computed value W_0 of the undistorted beam,

$$\Delta W = W_{\text{trial}} - W_0 \,.$$

The mean value and standard deviation of ΔW over the trials is shown as the last item in line three of the plot header.

6.2. Results

Figures 21-24 show the beam shape jitter characteristics for a 50×20 element array when the timing jitter at the elements varies from 100 ps to 1000 ps. In all cases, we assumed amplitude jitter 0.2 around the undistorted value of 1.0, (and normalized the amplitude power sum to unity). The beam width, in the xz-plane in this vertical pointing is $W = 0.68°$. This means that if we can accept $0.1 \times W$ errors in pointing, in essentially *no* simulation run, should ΔW exceed 0.07°. The panel (b) of the figures show that this requirement clearly is fulfilled for timing jitter up to 500 ps, but starts to become questionable at the timing jitter of 1000 ps. The changes in beam width are similarly small up to about 500 ps.

What is, perhaps, more troublesome is the loss of gain. At $\Delta t = 100$ *ps*, the mean loss of gain in the main beam is about 10% (0.5 dB), at $\Delta t = 300$ *ps* the loss is about 25% (1.3 dB) and at 500 ps about 50% (3.0 dB).

We emphasize that the loss of gain is mostly due to the "incohence" caused by the phase jitter. If we keep in the above four runs the input parameters otherwise intact but set the element amplitude jitter to zero, the beam jitter distributions change very little from those shown in Fig. 21-24. For example, the gain loss at 500 ps reduces from the 50% to about 44%.

Unless there is some fundamental problem with these simulation, it appears very clear that to get, say 0.1×beamwidth pointing accuracy, it is definitely enough to be able to control the element phase with something like 10–20° accuracy (clock timing with 100–300 pc accuracy at 225 MHz), as long as the phase errors at individual elements are uncorrelated. The large number of elements (1000 in this simulation) then takes care about averaging the distortions so that the main effect is just some loss of gain. The randomness of the timing/phasing errors at the elements is so important that it perhaps should be enforced.

7. SNR estimate for the test array

To get a rough estimate of SNR for the Kiruna test array, assume that the test array is oriented towards the VHF antenna, long size (the x-direction) towards the VHF antenna, and that the VHF antenna is perpendicular to that direction, at $x = L = 200$ km in the test array coordinate system, and assume that the line from the test array to the VHF antenna is perpendicular to the VHF vertical direction ("flat Earth"), see Fig. 25. Also, assume optimal polarization matching and assume that the angle χ between the

electric field and the scattering direction is constant over the whole common volume (in our case, it is then equal to the elevation angle ϵ from the test array to the center of the common volume). We use the bistatic radar equation to estimate the received signal power P_s

$$P_s = P_x \times \frac{\lambda^2}{(4\pi)^3} \frac{D_1 D_2}{R_1^2 R_2^2} \times \sin^2(\chi)\sigma_e \times n_e V_{\text{eff}} \,, \tag{93}$$

where the effective scattering volume is

$$V_{\text{eff}} = \int_{\text{CV}} dV(P) \frac{g_1(P) g_2(P)}{(r_1/R_1)^2 (r_2/R_2)^2} \,. \tag{94}$$

Quantities indexed by "1" refer to the VHF antenna system, quantities indexed by "2" refer to the test array system. The quantities g_1 and g_2 are the relative gains of the VHF antenna and the test array in the direction of the point P in the common volume, so that the absolutely normalized gains in the direction of P are $G_1(P) = D_1 \times g_1(P)$ and $G_2(P) = D_2 \times g_2(P)$. The relative gains are normalized to unity towards the center of the beams, the point Q.

For the vertical VHF beam, we use a gaussian beam shape approximation in the XY plane at altitude z

$$g_1(x, y) = \mathrm{e}^{-\frac{(x/r_1)^2}{A} - \frac{(y/r_1)^2}{B}} \,. \tag{95}$$

with $A = 3.97 \times 10^{-5}$ and $B = 3.19 \times 10^{-5}$, which correspond to half power beam width of 1.7° in the north-south ($= x$) direction, and 0.6° in the east-west ($= y$) direction, and $r_1^2 = x^2 + y^2 + z^2$. Eq. (95) is evaluated by SIMPLE_VHFBEAM.M in the package. We take the VHF antenna directivity to be $D_1 = 43.2$ dBi, which corresponds to an effective area of 3000 m^2.

The test array directivity D_2 as a function of the zenith angle of the phase-steered beam in the XZ-plane is computed by PLOT_MAXGAIN.M, which evalutes Eq. (71). For the array element gain, we use the simple approximation given by Eq. (73), with the element directivity 11.5 dBi. For the present purpose this seems a fair enough approximation of the gain diagrams provided by the element's manufacturer. The directivity D_2 is shown in Fig. 26. For the zenith angle 35° (elevation 55°), which correspond to the element Yagi maximum gain direction, and common volume center at 300 km above the VHF antenna, we find $D_2 = 28.1$ dBi. The relative gain g_2 of the test antenna is just taken to be the array factor AF squared, computed from Eq. (50) using ARRAYGAIN.M. The presumption is that an element's beam is wide compared to the arrays's grating lobe width. Fig. 28 shows the perpendicular cross section of the resulting test array beam shape g_2, projected to the common volume distance $R_2 = 360$ km, which corresponds to 300 km altitude. As marked in the figure, the half power beam width in the meridian plane is 3.7°.

The effective volume Eq. (94) is evaluted by COMMON_VOLUME.M by setting up a sufficiently tight rectangular grid of evaluation points which cover a sufficiently large 3D region around the common volume center point Q, and replacing the integral by the Riemann sum,

$$V_{\text{eff}} \approx \Delta V \times \sum_P \Gamma(P) \equiv \Delta V \times \sum_P \frac{g_1(P) g_2(P)}{[r_1(P)/R_1]^2 [r_2(P)/R_2]^2} \,. \tag{96}$$

where $\Delta V = dx\, dy\, dz$ is the volume of the grid's cell. We take the grid bounding box $\Delta X \times \Delta Y \times \Delta Z$ to be so large that it fully encompasses at least all the terms $\Gamma(P)$ that

are larger than 0.01. For the common volume at the altitude 300 km, a box with $\Delta X = 30$ km, $\Delta Y = 10$ km and $\Delta Z = 90$ km is large enough. With $dx = 0.3$ km, $dy = 0.1$ km and $dz = 0.5$ km, the grid has 1.85 million points. Without any attempt of optimization it takes about nine minutes by a 2 GHz Mac G5 to complete COMMON_VOLUME.M, returning $V_{\rm eff} = 1340$ km^3.

The program COMMON_VOLUME.M keeps all terms $\Gamma(P)$ of the sum in memory, together with the corresponding ranges $r_1(P)$ and $r_2(P)$. By binning $\Gamma(P)$ as a function of the pulse propagation delay $(r_1 + r_2)/c$, it is possible to inspect how the strength of the received signal increases as a function of time when the common volume is filled.[5] The top panel of Fig. 32 shows the filling of the scanttering volume by a long pulse, longer than about 600 μs. For a significantly shorter pulse, the volume is never fully filled, and the maximal signal strength is less. For instance, the standard EISCAT VHF experiment TAU1 uses an alternating code with 72 μs baud length. The bottom panel of Fig. 32, computed for a 70 μs pulse, shows that the maximum effective scattering volume is only 25% of the full volume when using the TAU1 illumination.

It is also possible to plot horizontal slices of the effective volume as contour plots of the value of $\Gamma(P)$ on the slice. An example is the horizontal slice through the center of the volume at altitude 300 km, shown in Fig. 33. The effective area

$$A = dxdy \sum_{P \in \text{slice}} \Gamma(P) \tag{97}$$

of the slice is 30 km^2. Fig. 33 plots the effective area as a function of altitude throughout the scattering volume.

By assuming electron density $n_e = 10^{11}$ m^{-3}, and using $P_x = 1$ MW, the expected signal power is estimated from Eq. (93) into Table 1 on p. 33, for three common volumes and for two pulse lengths. We assume 20 kHz receiver bandwidth, as in TAU1 for VHF, and system temperature 150 K, to estimate the noise power and then find the SNR values as shown in Table 1:

1. **For the common volume at 120 km** we predict a SNR of about 9% when transmission uses a long enough pulse ($\gtrsim 300$ μs) to fill the volume, and about 4% for a 70 μs pulse.

2. **For the common volume at 300 km** we predict a SNR of 22% when transmission uses a pulse long enough ($\gtrsim 500$ μs) to fill the volume, and 6% for a 70 μs pulse.

3. **For the common volume at 600 km** we predict a SNR of 27% when transmission has a pulse long enough ($\gtrsim 1500$ μs) to fill the common volume, and 2% for a 70 μs pulse.

We note that in the case of volume-filling pulses, the larger common volume size compensates the larger distances, but that this is not the case for a short pulse of a fixed length. We also note that SNR is smaller for the 120 km altitude volume than in the higher volumes mainly because of the substantially smaller polarization factor.

[5] The points of constant propagation delay define a scattering surface, an ellipsoidal surface slicing the common volume. For a very short transmitted pulse, at any instant of time, the received signal is the sum of all the rays scattered through the surface. It is the area of this surface, times its (small) thickness, that defines the volume element that is relevant when inspecting how the whole volume is filled. Rather than computing the volume analytically, COMMON_VOLUME.M just picks all those points $\Gamma(P)$ that have the propagation delay in a given small interval of time.

Table 1: Predicting SNR for the test array. We use Eq. (93), for three common volume altitudes: 120 km, 300 km and 600 km, and two pulse lengths: a volume-filling long pulse (LP) and a 70 μs pulse. We use constant electron density $n_e = 10^{11}$ m^{-3}, and make no temperature correction to the electron scattering cross section $\sigma_e = 10^{-28}$ m^2. The main work in the computation is to estimate the effective scattering volume $V_{\rm eff}$, using Eq. (96). Transmission power 1 MW and optimal polarization matching are assumed. For the noise power, we use system temperature 150 K, assume receiver bandwidth $B = 20$ kHz, and estimate the power as $P_{\rm noise} = k_{\rm B} T_{\rm sys} B$. In the package, the SNR is computed by TESTARRAY_SNR.M, using effective volumes computed by COMMON_VOLUME.M.

P_x	1×10^6 W	1×10^6 W	1×10^6 W
R_1	**120 km**	**300 km**	**600 km**
n_e	1.0×10^{11} m^{-3}	1.0×10^{11} m^{-3}	1.0×10^{11} m^{-3}
ϵ_2	30°	55°	70°
R_2	233 km	363 km	634 km
χ	32°	57°	72°
$\sin^2 \chi$	0.28	0.67	0.88
$V_{\rm eff}$ LP	155 km^3	1340 km^3	13600 km^3
$V_{\rm eff}$ 70 μs	67 km^3	342 km^3	1250 km^3
$G_{\rm e}$	11.5 dBi	11.5 dBi	11.5 dBi
D_1	43.2 dBi	43.2 dBi	43.2 dBi
D_2	25.4 dBi	28.0 dBi	28.5 dBi
$P_{\rm s}$ LP	3.61×10^{-18} W	9.24×10^{-18} W	11.0×10^{-18} W
$T_{\rm sys}$	150 K	150 K	150 K
B	20 kHz	20 kHz	20 kHz
$P_{\rm noise}$	4.14×10^{-17} W	4.14×10^{-17} W	4.14×10^{-17} W
SNR LP	**0.09**	**0.22**	**0.27**
SNR 70 μs	**0.04**	**0.06**	**0.02**

A. Figures to Chapters 2–7

Listing of the figures the is on p. 3. There are a few more figures in this compilation than are referred to in the main text. Also, there are considerable amount of details, both in the figures and in their captions, that are not handled elsewhere in the notes. For many of figures we indicate the Matlab M-FILES in the E3ANT package that were used to generate them.

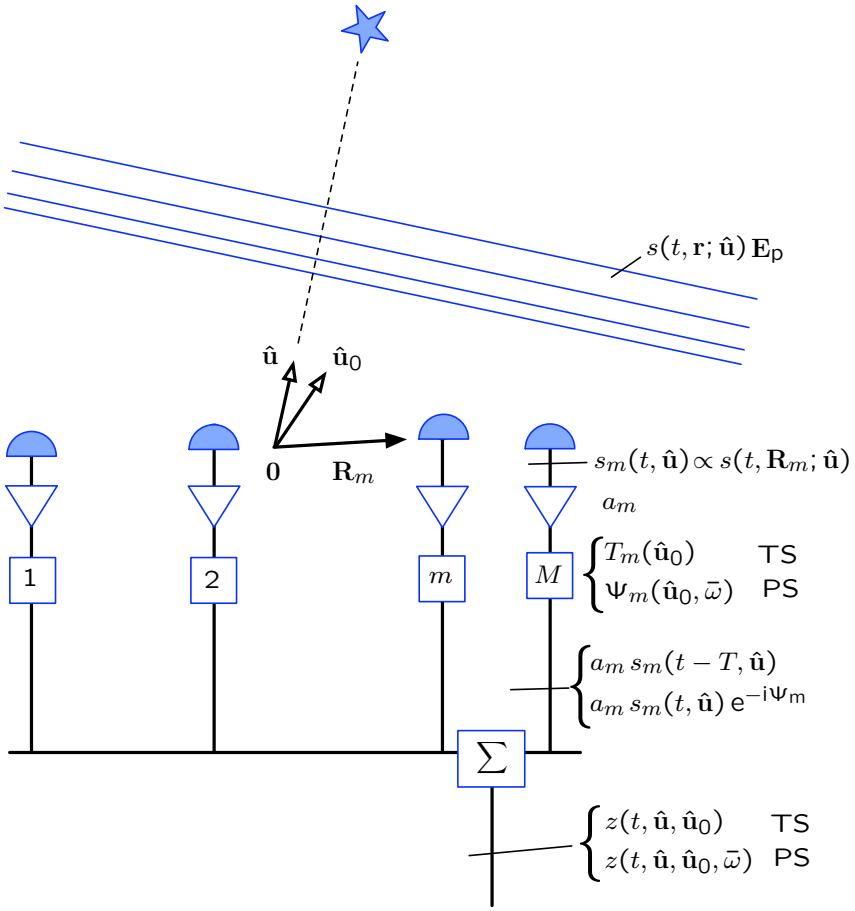

Figure 1: Beam steering, reception view in the continuous-time domain. A far-away point source in direction $\hat{\mathbf{u}}$ produces time- and space varying incoming electric field $s(t, \mathbf{r}, \hat{\mathbf{u}})\mathbf{E}_\mathrm{p}$ near the antenna array of M elements. The vector $\mathbf{E}_p$ is taken to be complex-valued to represent polarization; it may depend on the direction $\hat{\mathbf{u}}$, but not on the position $\mathbf{r}$ or the time t. The elements sniff the incoming field at points $\mathbf{R}_m$ so that a (complex-valued, to represent the polarization) voltage $s_m(t)$ is generated across the terminals of element m. This voltage is amplified by a real factor a_m and fed to the beam-former system, which may be either a time-steering system (TS) or a phase-steering system (PS). In the TS system, the signal $a_m s_m$ at element m is delayed by an amount T_m which depends on the element position and the desired steering direction $\hat{\mathbf{u}}_0$, before being fed to an adder which produces the final beam-formed signal $z(t)$. In the PS version of the beam-former, there is no explicit delaying, but instead the phase of $a_m s_m(t)$ is adjusted by an angle Ψ_m, computed from the element position, the desired beam direction, and the average frequency $\bar{\omega}$ of the incoming pulse. The figure represents the array elements by semi-spheres to suggest an isotropic element gain in the upper half-sphere. When desired, a non-isotropic element power gain $\mathrm{g_E}$ can be explicitly incorporated by replacing a_m by $a_m \sqrt{\mathrm{g_E}(\hat{\mathbf{u}})}$.

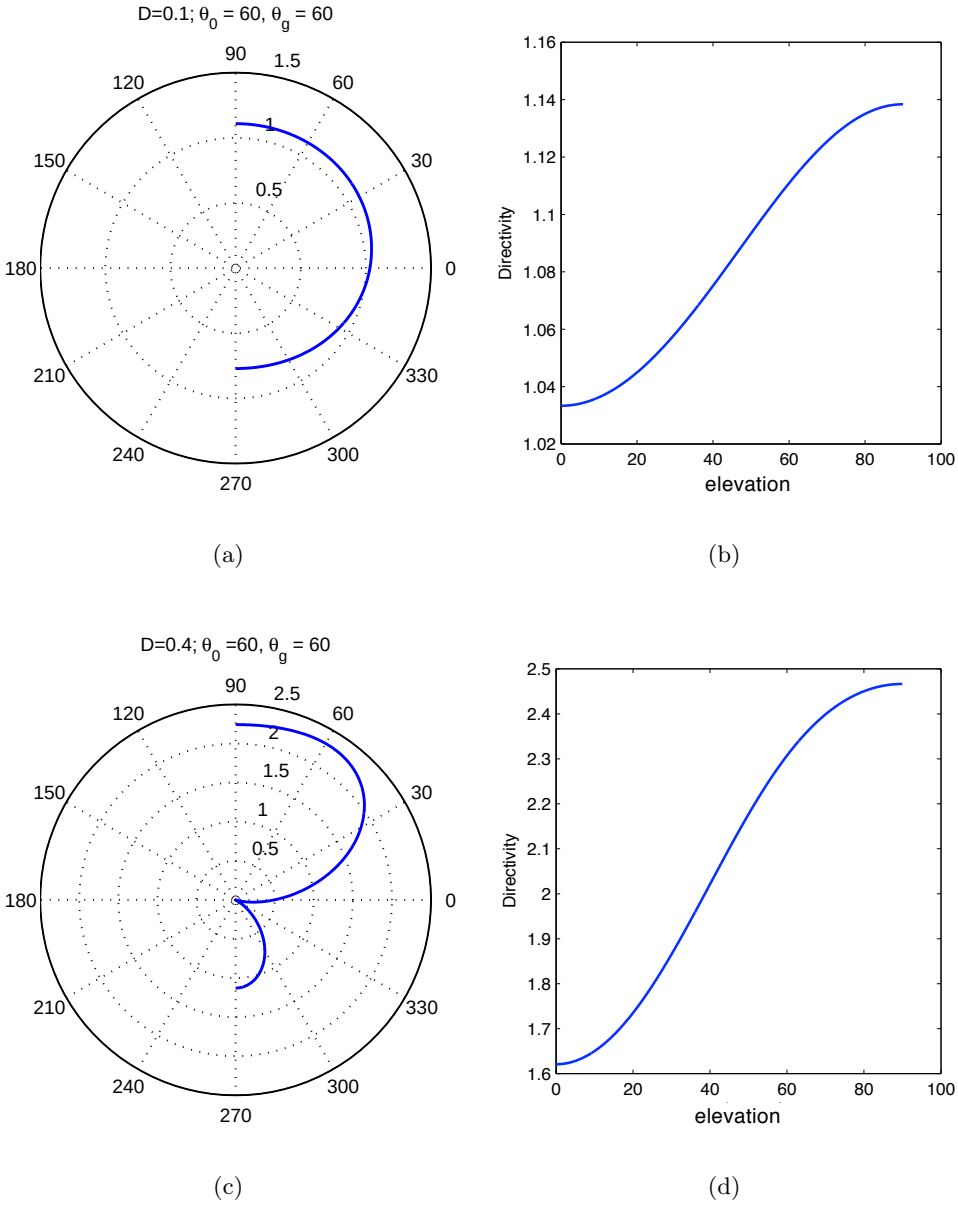

Figure 2: Gain pattern and directivity of an vertical array of two isotropic elements. Panels (a) and (b) are for element separation $d = 0.1\lambda$, panels (c) and (d) are for $d = 0.4\lambda$. The beam steering in panels (a) and (c) has been to 60° from boresight (horizontal beam). The 3D gain pattern is obtained from the curves shown by rotating them around the vertical axis, which is also the direction of the array axis. The polar plots are labeled by the beam elevation angle, and the gain is in absolute units. Both of these arrays are dense ($D < 0.5\lambda$), so there are no grating lobes apart the main lobe, but there nevertheless is a rather well-developed ordinary side lobe in (c).

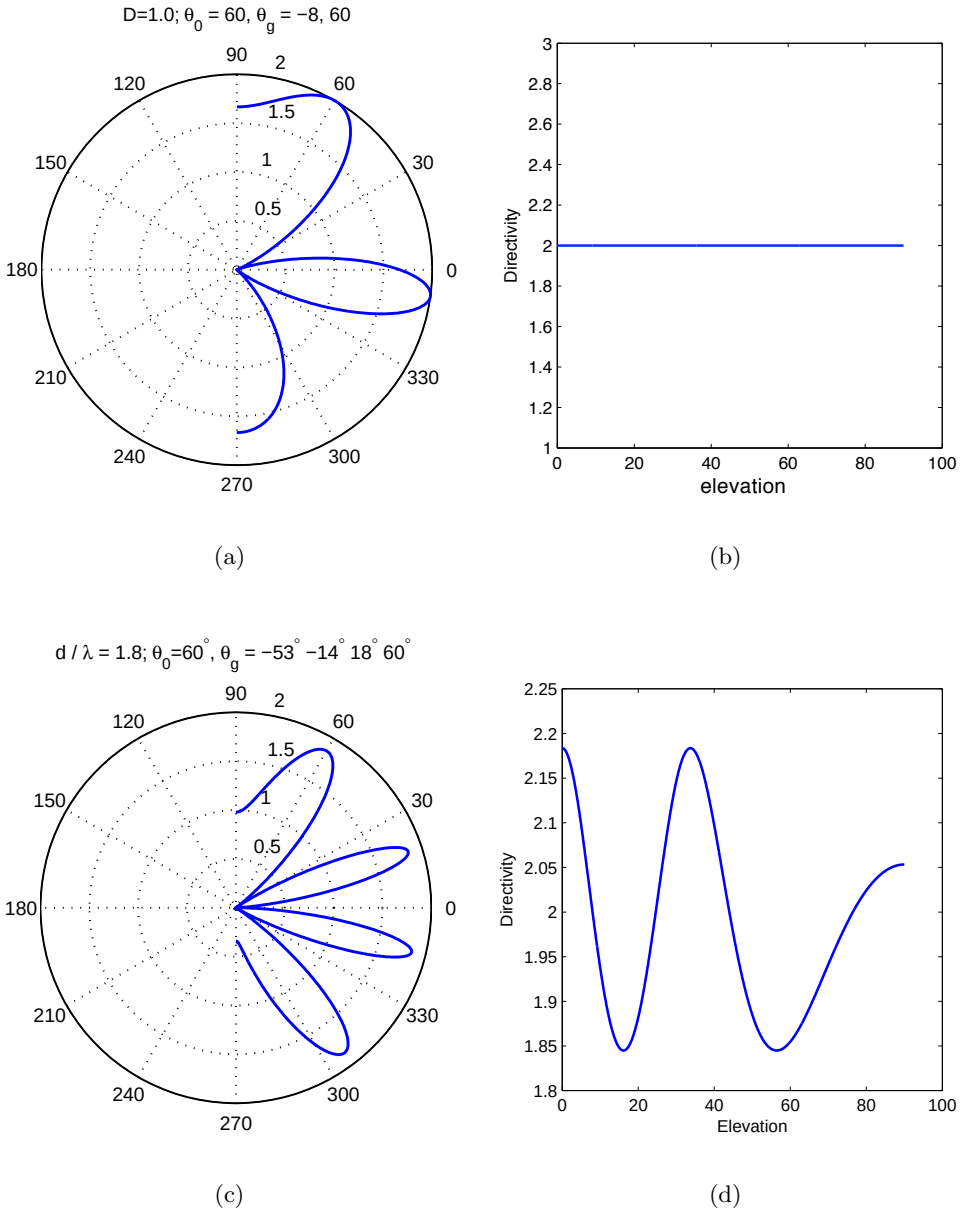

Figure 3: Gain pattern and directivity of an vertical array of two isotropic elements. Panels (a) and (b) are for element separation $d = 1.0\lambda$, panels (c) and (d) are for $d = 1.8\lambda$. The beam steering in panels (a) and (c) has been to 60° from boresight (horizontal). The 3D gain pattern is obtained from the curves shown by rotating them around the vertical axis, which is also the direction of the array axis. The polar plots are labeled by the beam elevation angle, and the gain is in absolute units. In (a), there are two grating lobes and one ordinary, but large, side-lobe, while in (c), all the lobes have equal directivity, and are grating lobes.

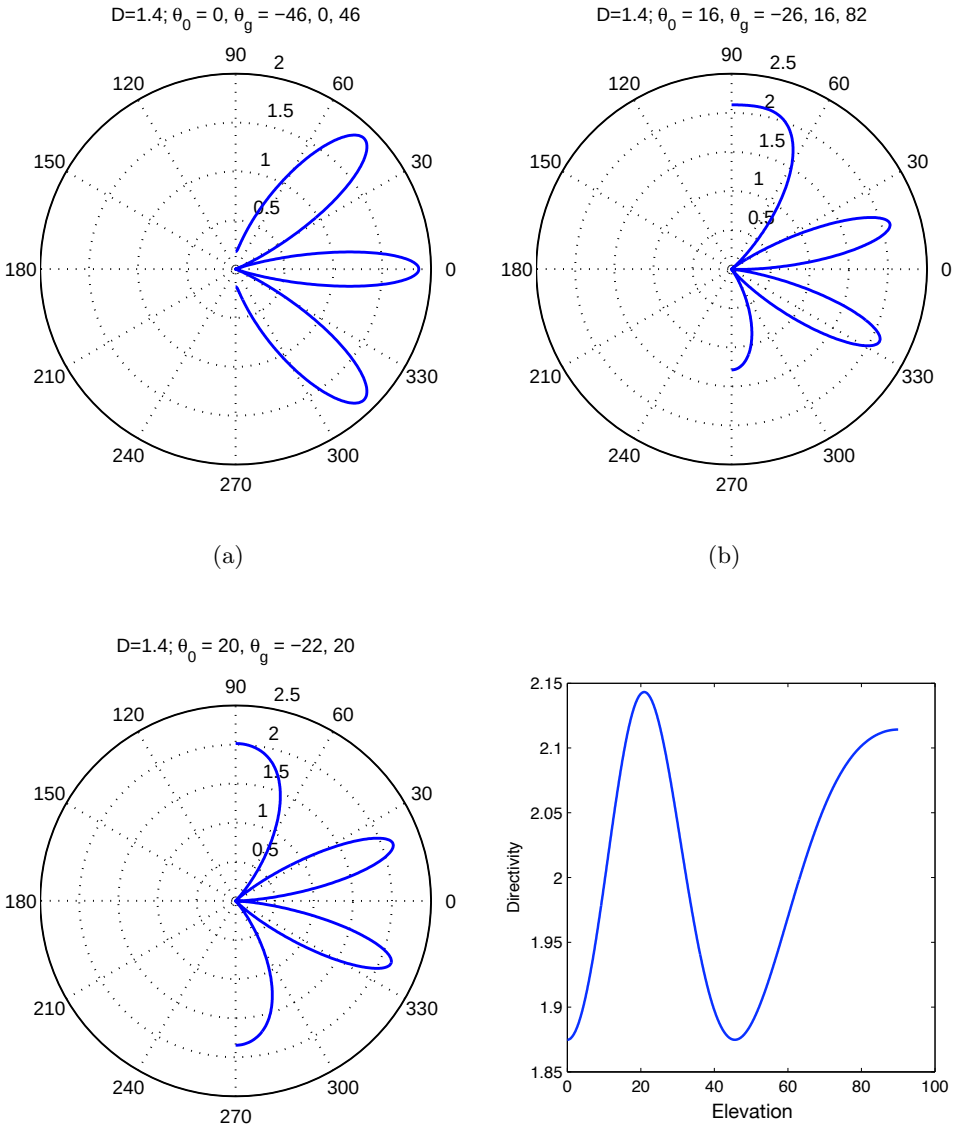

(a) (b) (c) (d)

Figure 4: Gain pattern and directivity of an vertical array of two isotropic elements. Element separation is $d = 1.4\lambda$. Beam steering is to 0° (horizontal) in panel (a), to elevation 16° in (b) and to 20° in (c). In (a), all the three lobes are grating lobes, in (b), there are three grating lobes, and in (c), only two grating lobes. As function of the steering angle, the directivity oscillates around the value 2, the absolute maximum value 2.14 is achieved with the steering angle 20.9°.

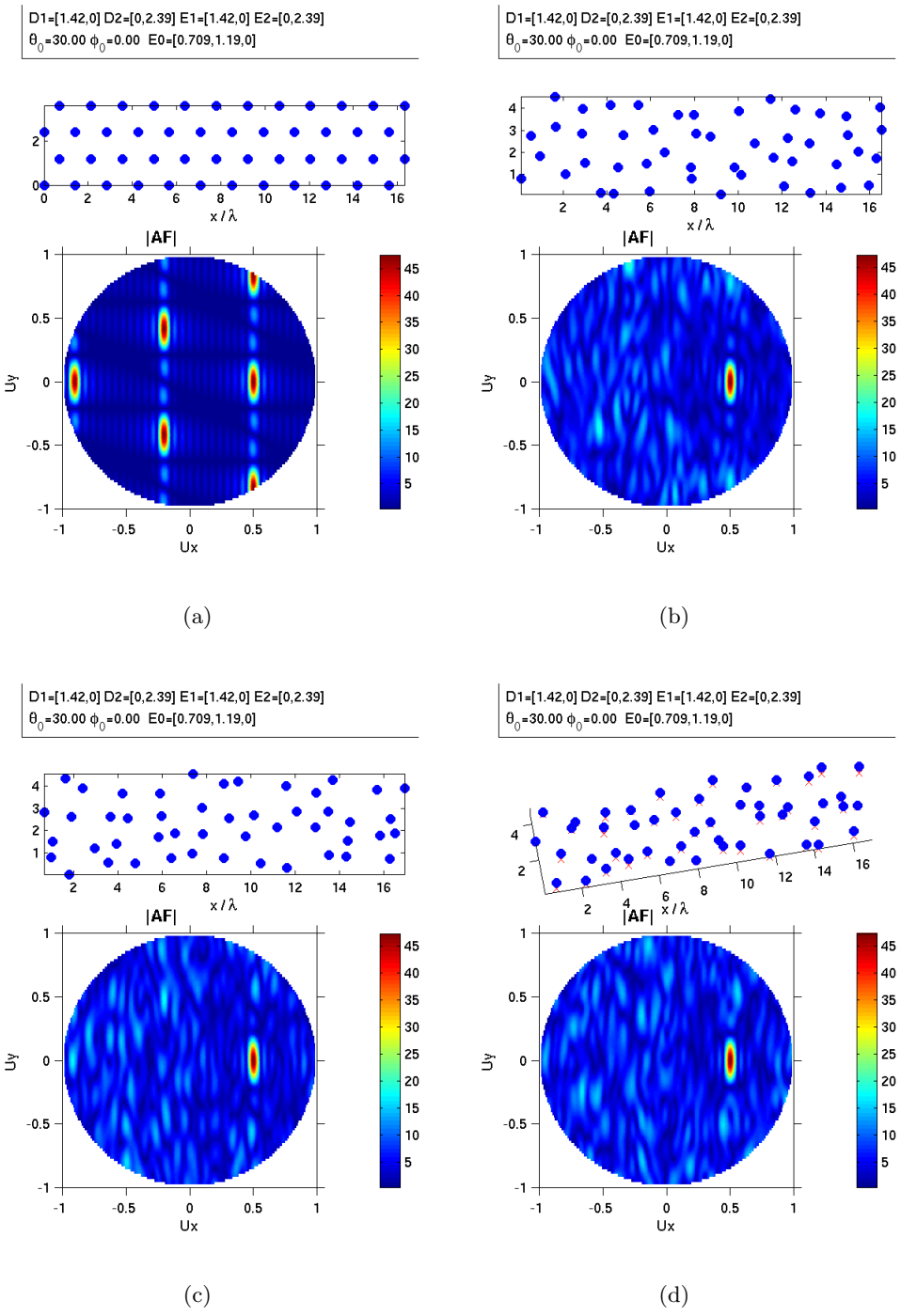

Figure 5: Randomizing array element positions. Panel (a) shows the array factor $\hat{\mathbf{u}} \mapsto \mathrm{AF}(\hat{\mathbf{u}} - \hat{\mathbf{u}}_0)$ for a 12×4 regular planar array with isotropic elements. The array has been phase-steered to 60° elevation. Panels (b) and (d) shows two randomizations, where the grid positions in x- and y-directions have been increased by a random amount, uniformly distributed between 0 and one wavelength. In panel (d), also the z-position has been similarly randomized.

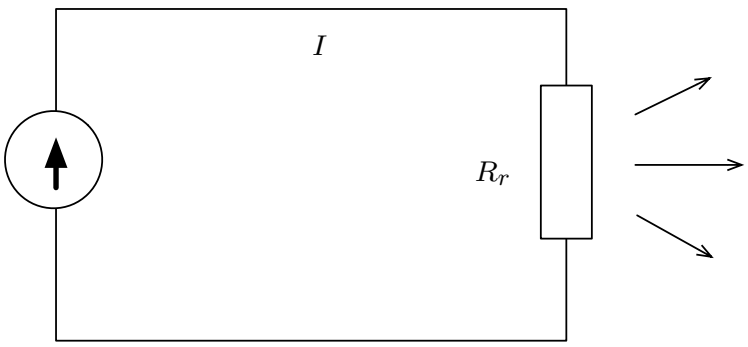

Figure 6: TX equivalent circuit.

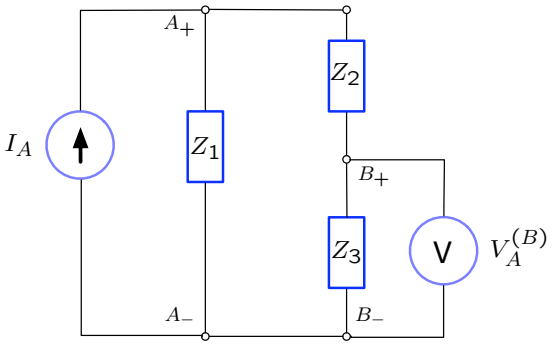

(a)

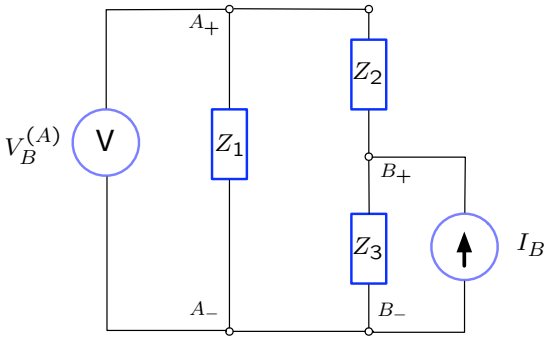

(b)

Figure 7: Reciprocity in electronic circuitry. Assume that in panel (a), a current $I_A = I_0$ is applied to port A of a two-port circuit, and that it causes the voltage $V_A^{(B)} = U_0$ in port B. Then assume that the current generator and the voltmeter are interchanged, to get the situation shown in panel (b). Assume that the generator is adjusted so that it produces the same current I_0 to port B, $I_B = I_0$. Then the statement of reciprocity is that the voltage meter at port A will read U_0, $V_B^{(A)} = U_0$. For the specific circuitry shown here, this can be verified by direct computation of the voltage, which in both cases gives $U_0 = Z_{AB} I_0$, where $Z_{AB} = Z_1 Z_3/(Z_1 + Z_2 + Z_3)$. The internal currents and voltages in cases (a) and (b) are different—for instance, the currents through Z_2 and Z_3 are equal in case (a) and non-equal in case (b)—but the *coupling* between the ports is the same; in both cases, it is quantified by the same linear relationship involving the impedance Z_{AB}.

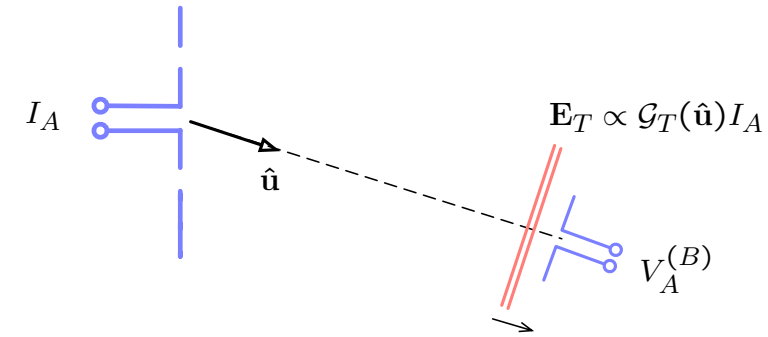

(a) *Transmission from A.*

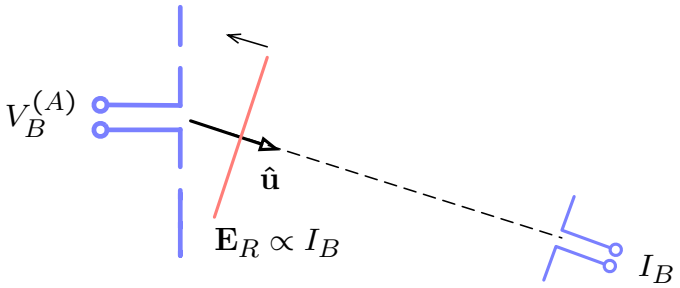

(b) *Transmission from B.*

Figure 8: Antenna directional gain in reception. A small test antenna, e.g. a short dipole, is at a fixed distance from the antenna of interest, always oriented perpendicularly to the direction unit vector $\hat{\mathbf{u}}$. We envision $\hat{\mathbf{u}}$ but not the distance to be varied by moving the test antenna, while always keeping it perpendicular to $\hat{\mathbf{u}}$, and inquiry the dependency on $\hat{\mathbf{u}}$ of the voltage $V_B^{(A)}$ at A caused by the current at B, the situation shown in panel (b). We first consider the transmission from A as in panel (a). Total transmitted power is proportional to I_A^2, so by definition of the directional amplitude gain $\mathcal{G}_T(\hat{\mathbf{u}})$, the far field $\mathbf{E}_T$ in direction $\hat{\mathbf{u}}$ is proportional to $\mathcal{G}_T(\hat{\mathbf{u}})I_A$. On the other hand, the induced voltage $V_A^{(B)}$ depends linearly on $\mathbf{E}_T$, so that also $V_A^{(B)}$ is proportional to I_A and $\mathcal{G}_T$. We write this as $V_A^{(B)} = Z_{AB}I_A$, where $Z_{AB} = a\,\mathcal{G}_T(\hat{\mathbf{u}})$ and the factor a that does not depend on $\hat{\mathbf{u}}$. By reciprocity, the impedance Z_{AB} gives also the coupling from B to A in panel (b): $V_B^{(A)} = a\,\mathcal{G}_T(\hat{\mathbf{u}})\,I_B$. The (linear) relation between $\|\mathbf{E}_R\|$ and I_B cannot depend on $\hat{\mathbf{u}}$, so we must also have $V_B^{(A)} = b\,\mathcal{G}_T(\hat{\mathbf{u}})\,\|\mathbf{E_R}\|$, with some b that is independent of $\hat{\mathbf{u}}$. That is, all directional dependency in $V_B^{(A)}$ comes via $\mathcal{G}_T(\hat{\mathbf{u}})$. This shows that the gain pattern in reception is equal to the gain pattern in transmission. To find the constants of proportionality a and b requires knowledge of the actual radiation fields associated with a short dipole. With standard assumptions of polarization and impedance matching in the receiving system, this leads to the general result $A_{\text{eff}} = (\mathcal{G}_T(\hat{\mathbf{u}}))^2\lambda^2/4\pi$ for the effective area of an receiving antenna.

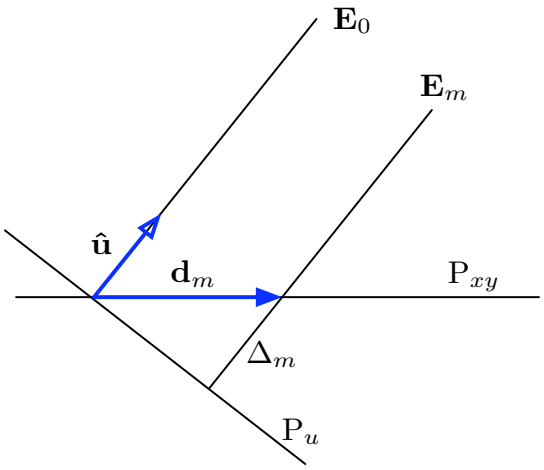

Figure 9: Computing the time delay/the phasing factor for an array element . We are interested in computing the far field of an antenna array in the direction $\hat{\mathbf{u}}$, when the array elements are at the positions $\mathbf{R}_m$. The plane P_u is normal to $\hat{\mathbf{u}}$. For a monochromatic plane wave, the relative phases of the fields $\mathbf{E}_m$ are equal to the elements' phase distances $2\pi\Delta_m/\lambda$ from this plane. The time distance is $T_m = \Delta_m/c$, independent of the wave length.

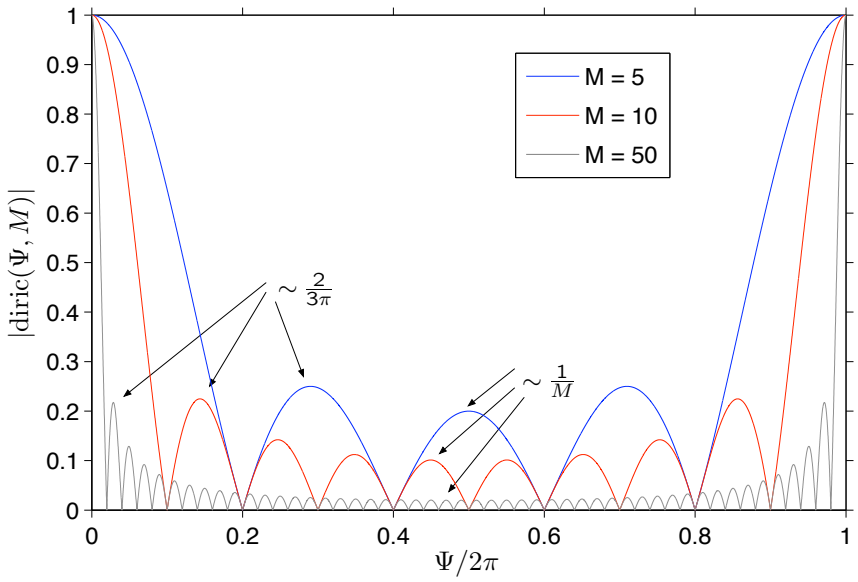

Figure 10: Magnitude of the Dirichlet kernel for three values of the M-parameter. The value of the largest local maxima, located at about $\Psi \approx 3\pi/M$ and $\Psi \approx 2\pi - 3\pi/M$, and the smallest local maximum, is indicated. The largest maximum has value of about 0.212 (-13.5 dB in terms of power), roughly independent of M for any larger M, while the smallest maximum, near $\Psi \approx \pi$, goes towards zero as 1/M. The kernel has zeros at the points $\Psi = 2\pi n/M$.

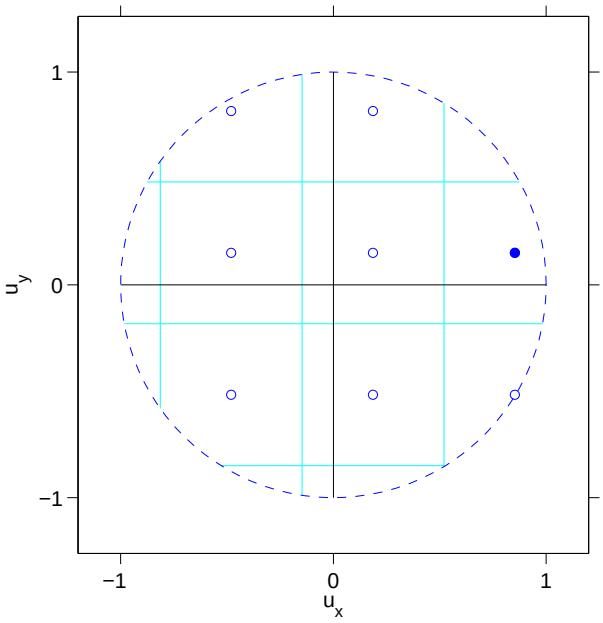

Figure 11: Grating zones of an regular, rectangular plane array. The element spacing is $D_x = D_y = 1.5$. The array is phase-steered so that the beam of zone Z(1,0), the solid dot, points to $\phi = 10.0°$, $\theta = 60.0°$. The unwrapped phasing angles are $\delta_x = 460.5°$, $\delta_y = 81.2°$.

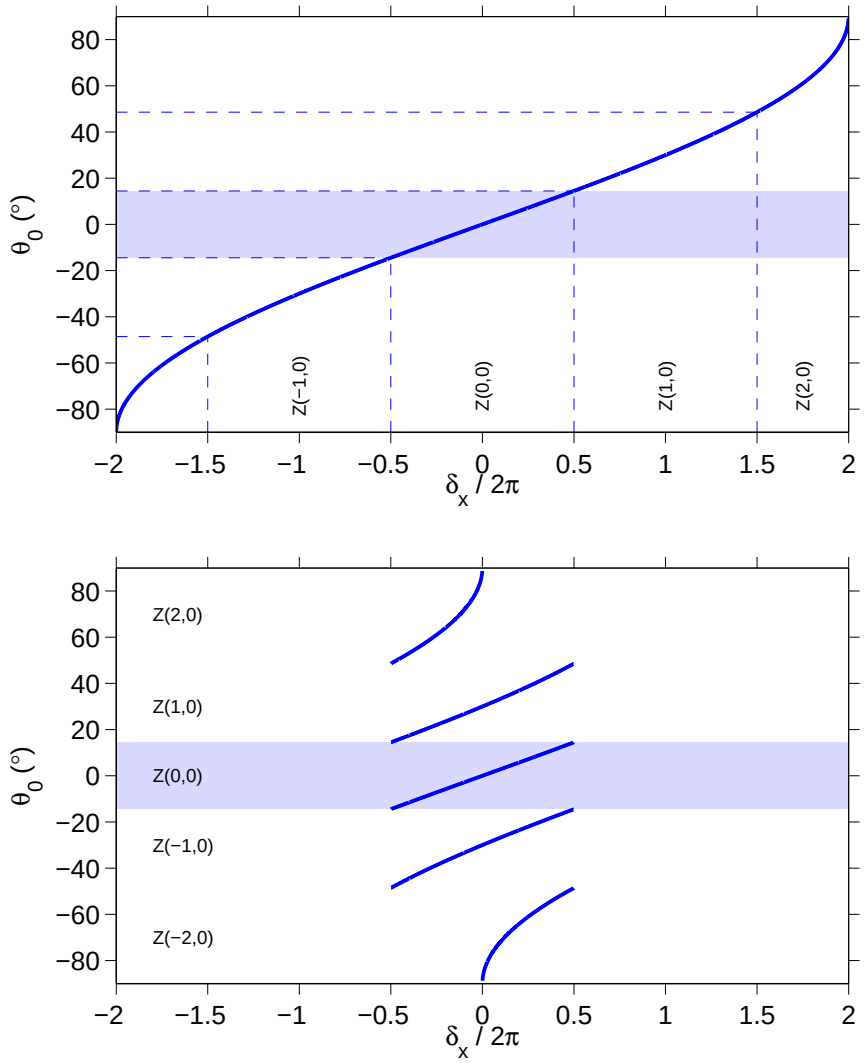

Figure 12: Beam polar angle as function of the element-to-element phase step. The element spacing is $D_x = 2.0$. In the top panel, the phase step δ_x is computed from $\delta_x = 2\pi D_x u_x$, in the bottom panel, δ_x has been shifted to the interval $[-\pi, \pi[$. The beams' grating zones are also indicated. Note the non-linear dependence of θ_0 on δ_x. The top panel is perhaps the better choice when focusing on a single beam when it moves through the full range of pointing directions. The bottom panel instead emphasizes the in fact there are a set of equivalent grating beams, which are all steered simultaneously. The plots were produced by BEEMSTEERING.M.

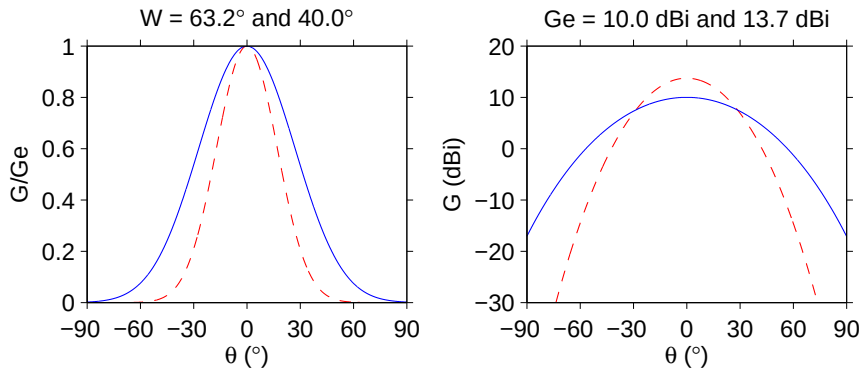

Figure 13: The $\cos^n(\theta/2)$ gain pattern. The left panel shows the gain in linear units, the right panel in dBi. The blue solid line represents a beam with directivity 10.0 dBi and beam-width 63.2°. The dashed red line represents a beam with directivity 13.7 dBi and beam-width 40.0°.

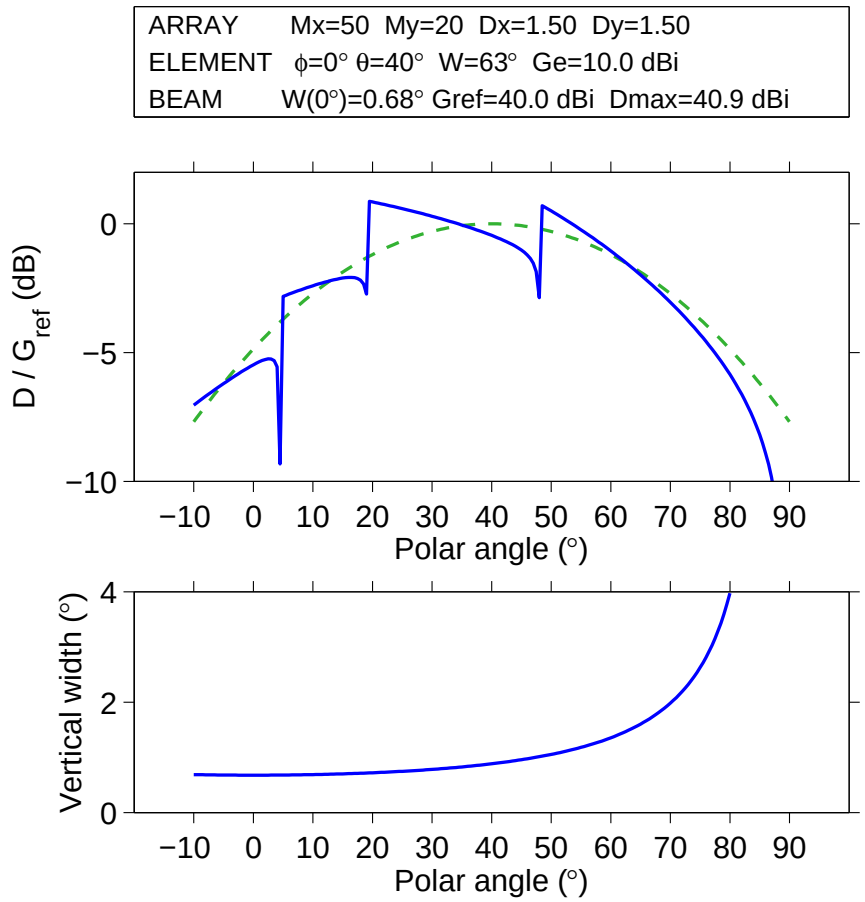

Figure 14: Directivity and vertical beam width of an array. The 50×20, 1.5×1.5 rectangular plane array uses 10 dBi elements, tilted 40° from the vertical. The directive has been normalized by the arrays reference gain. In addition to the directivity, the top panel shows the element's gain pattern, normalized to unity at its maximum. All the plots are for the vertical plane that contains the element's direction. The figure was produced with PLOT_MAXGAIN.

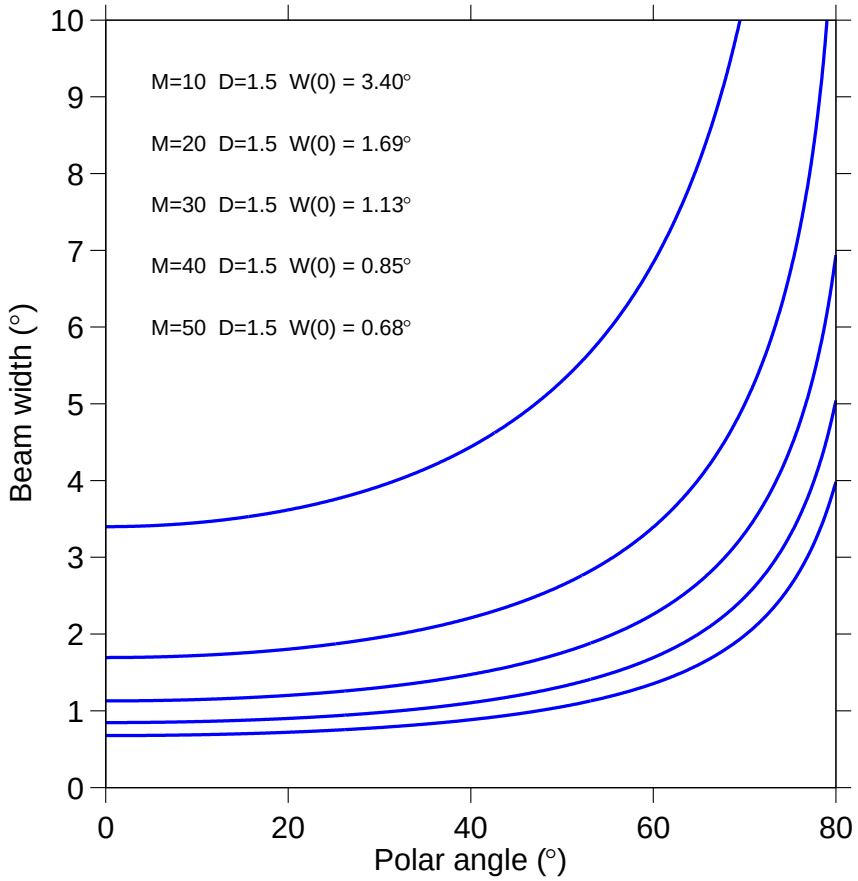

Figure 15: Beam width for a few sizes of a linear array. Element spacing is 1.5 wavelengths. The number of elements M and the beam width to bore-sight direction $W(0)$ are given in the legend.

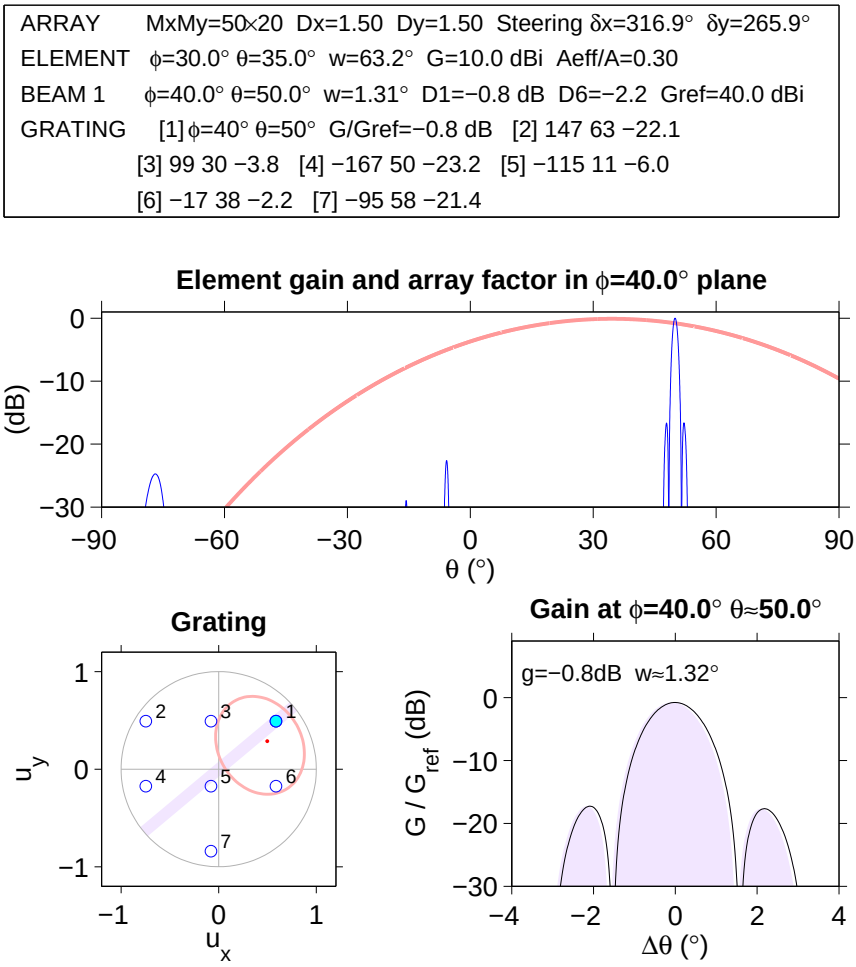

Figure 16: Inspecting the array pattern with PLANEARRAY.

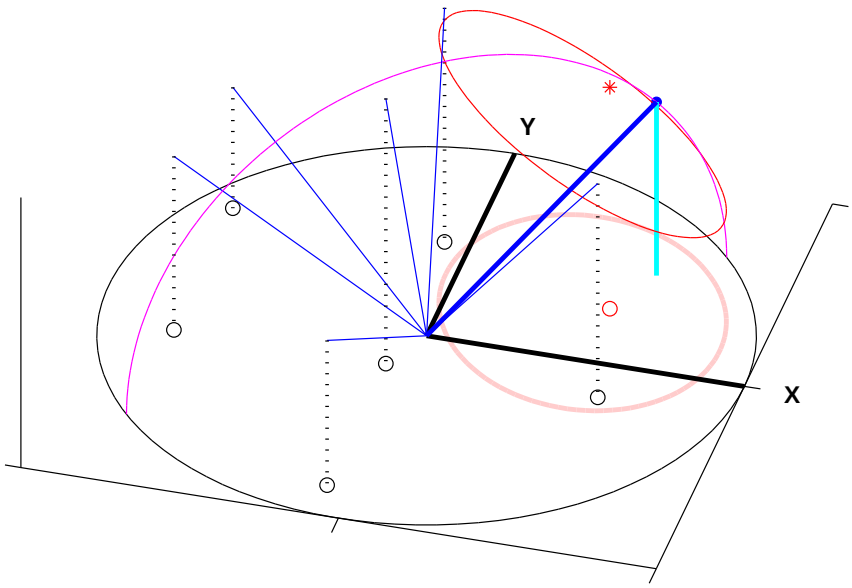

Figure 17: A 3D view of an array's grating directions. This figure was produced by PLANEARRAY, with parameters as in Fig. 16.

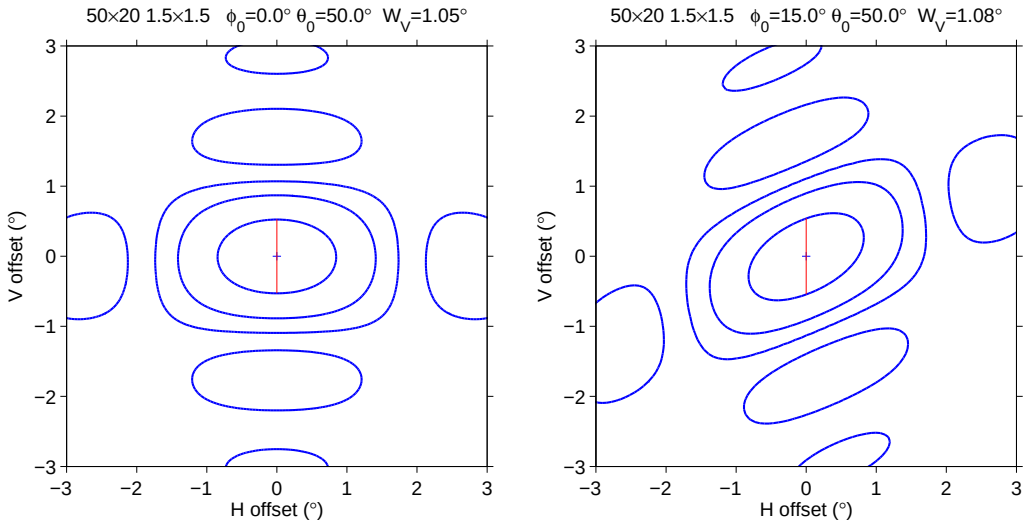

(a) (b)

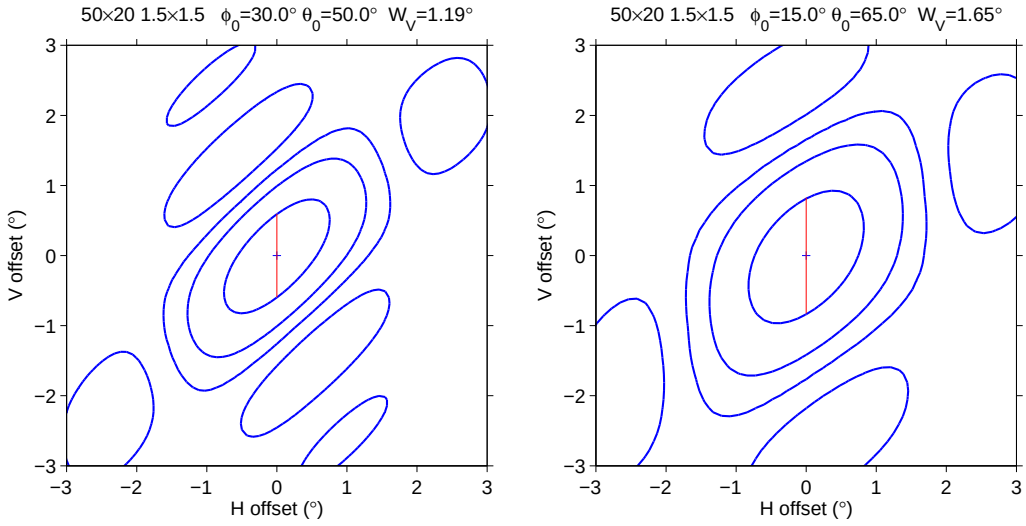

(c) (d)

Figure 18: Shape of an array's beam cross section . Panels (a)-(c) are for elevation 50°, panel (d) for elevation 25°. The rectangular plane array has size $M_x = 50$, $M_y = 20$ elements, with uniform element spacing of 1.5 wavelengths. The contour plot shows the beam power gain at the 0.5, 0.1 and 0.01 levels compared to the beam center. The plotted cross section is perpendicular to the beam axis, with the plot x-axis in the horizontal plane; that is, the view is as seen along the beam axis, away from the radar. The plots were produced by BEAMSHAPE2D.M.

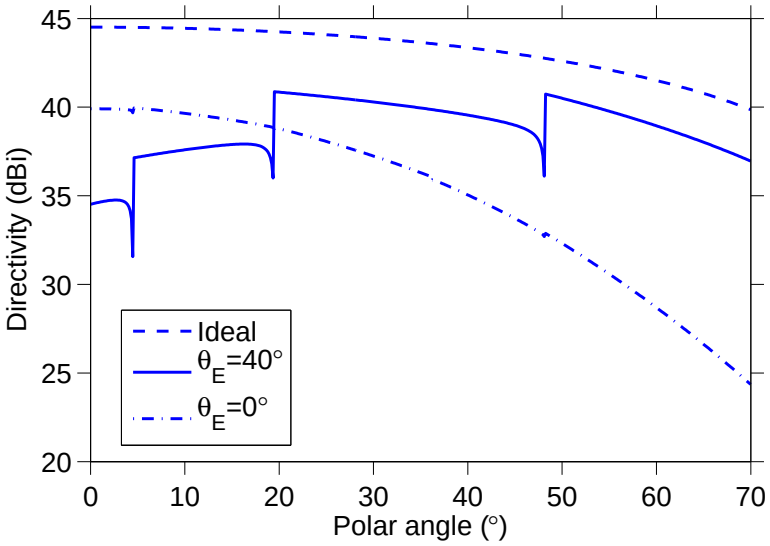

Figure 19: Narrow dips in the array directivity pattern. The figure shows the directivity of an 50×20 array, with 1.5 wavelength spacing, in the vertical plane through the elements' direction. The element has gain $G_e = 10$ dBi. Both the curve for vertical elements and elements tilted by 40° are shown. Also is shown the directivity of a dense ($D < 0.5$) array of the same physical boundary.

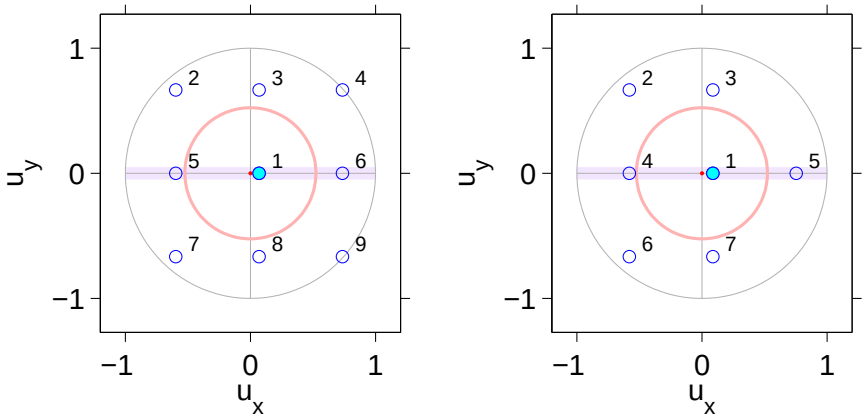

(a) $\theta_1 = 4.0°$, $g_4 = g_9 =$ -23 dB

(b) $\theta_1 = 5.0°$

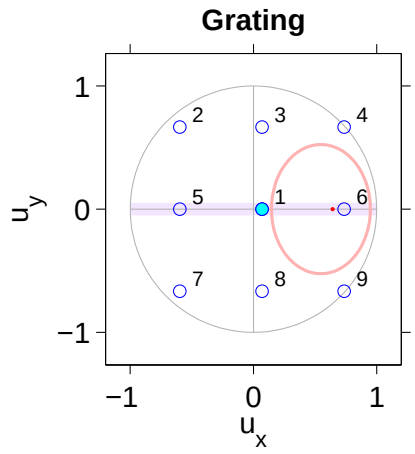

(c) $\theta = 4.0°$, $g_4 = g_9 =$ -11 dB

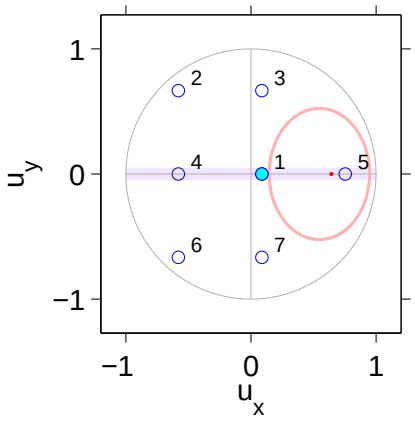

(d) $\theta_1 = 5.0°$

Figure 20: Explaining the directivity dips. This figure illuminates the origin of the dip at $\theta \approx -4.5°$ in the directivity curves of Fig. 19. In panels (a) and (b), the array elements are vertical, in panels (c) and (d), the elements have been tilted to $\phi_E = 0, \theta_E = 40°$. When the marker beam (beam 1) is phase-steered from 4° to 5°, two grating beams move out of the circle of visibilitity. For the tilted elements, a still significant amount of power is suddenly taken and then re-released, for the gain of both the horizontal beams is still only about 10 dB down from the main beams. Instead, for the vertical elements, beams 4 and 9 have so little gain that what they do near the boundarary of the visibility circle does not matter in the power budget. The figure was produces with PLANEARRAY.

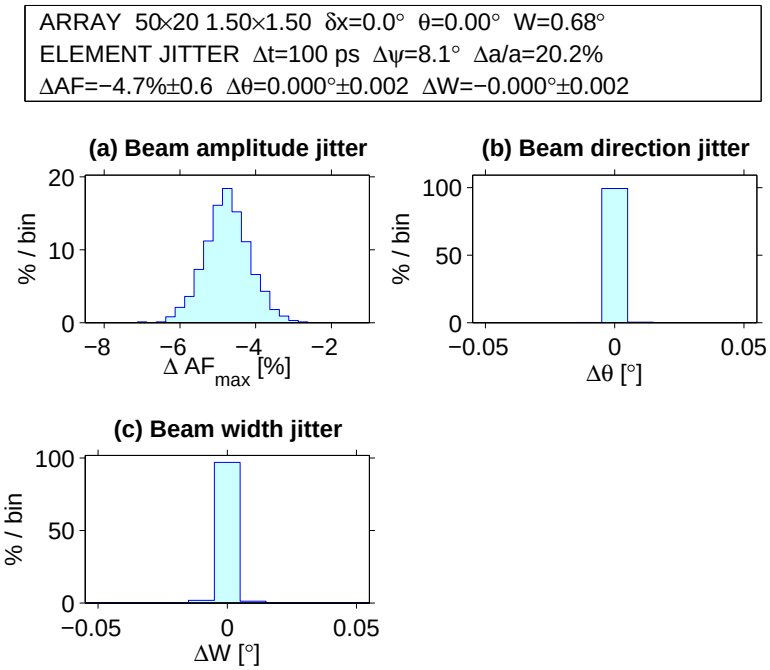

Figure 21: Jitter simulation 1. Simulated array factor jitter in a 50×20 element array in x-direction, when element timing jitter is $\Delta t = 100$ ps, the corresponding element phase jitter 8.1°, and the element amplitude jitter is 20% around 1. The undistorted beam has been directed in vertical direction, and has half-power width of 0.68° in the x-direction.

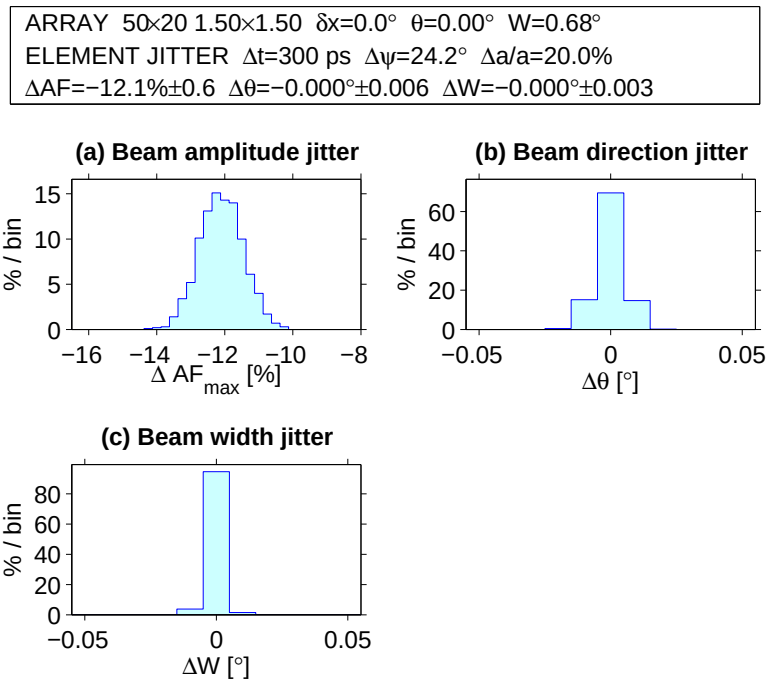

Figure 22: Jitter simulation 2. Simulated array factor jitter in a 50×20 element array in x-direction, when element timing jitter is $\Delta t = 300$ ps, the corresponding element phase jitter 45°, and the element amplitude jitter is 20% around 1. The undistorted beam has been directed in vertical direction, and has half-power width of 0.68° in the x-direction.

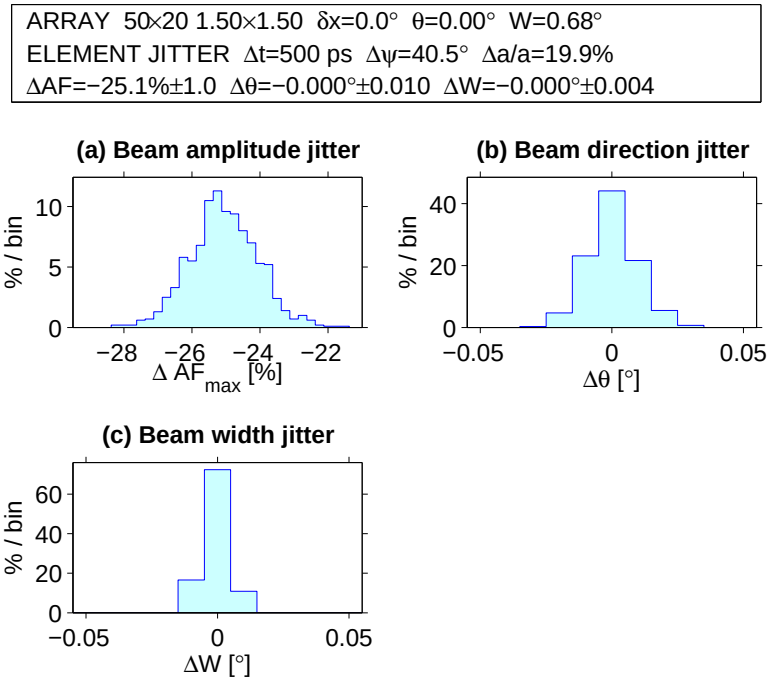

Figure 23: Jitter simulation 3. Simulated array factor jitter in a 50×20 element array in x-direction, when element timing jitter is $\Delta t = 500$ ps, the corresponding element phase jitter 24°, and the element amplitude jitter is 20% around 1. The undistorted beam has been directed in vertical direction, and has half-power width of 0.68° in the x-direction.

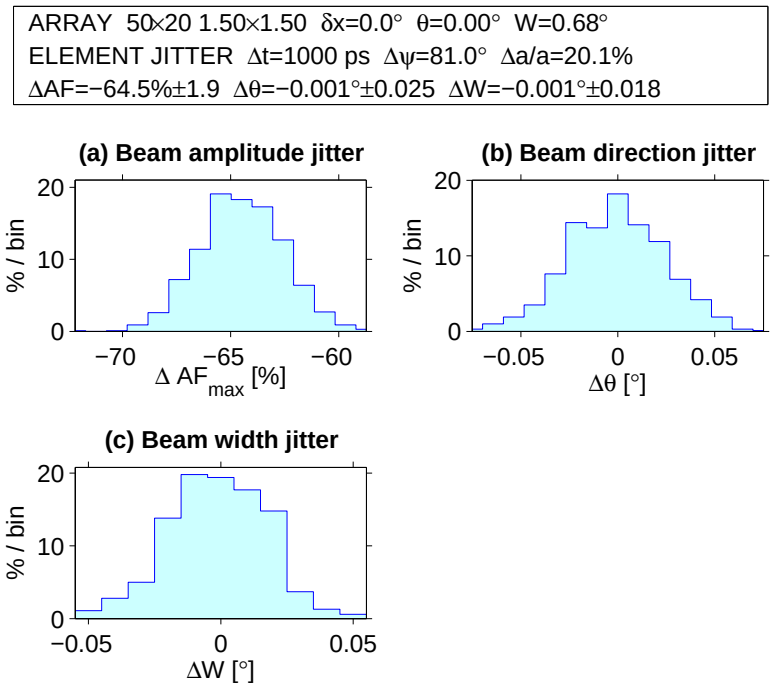

Figure 24: Jitter simulation 4. Simulated array factor jitter in a 50×20 element array in x-direction, when element timing jitter is $\Delta t = 1000$ ps, the corresponding element phase jitter 81°, and the element amplitude jitter is 20% around 1. The undistorted beam has been directed in vertical direction, and has half-power width of 0.68° in the x-direction.

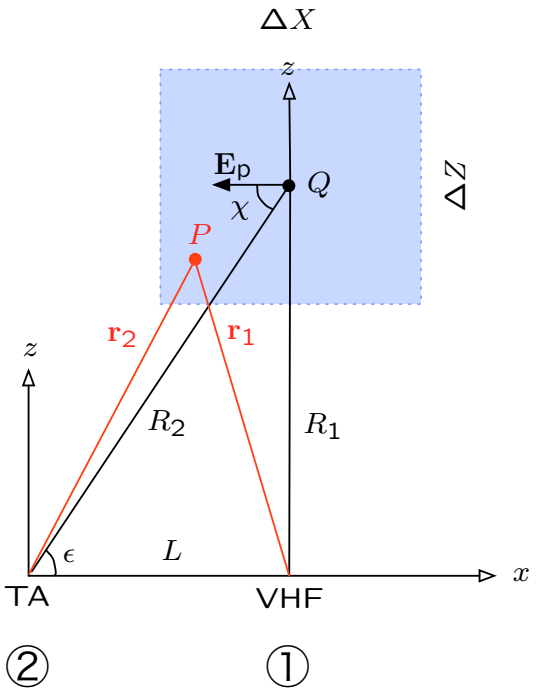

Figure 25: TA: Geometry for computing the effective volume. We make two simplifications to the actual geometry. First, we assume flat Earth. Second, we assume that the VHF antenna rotation axes is along the y-axis in the figure, that is, perpendicular to the line from TA to the VHF antenna, which is our x-axis. The effective volume is computed using Eq. (96). Q is the center point of the common volume. P is a point in the computation grid. The angle χ is the angle between the polarization vector and the direction of the scattered wave. We did, by oversight, take χ to be constant over the whole computation grid. We did let the distances r_1 and r_2 to vary in the proper way, though.

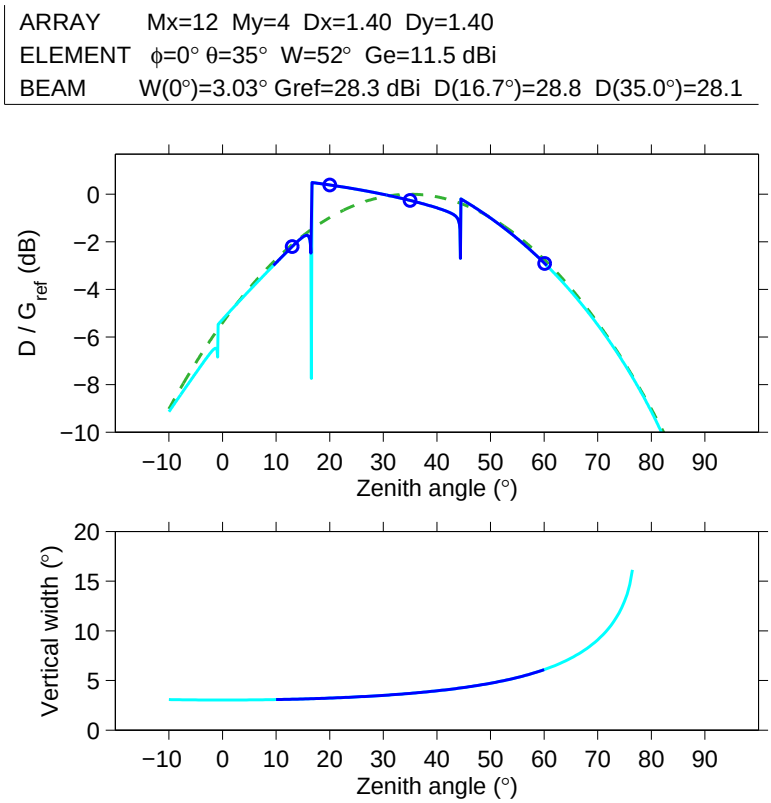

Figure 26: TA: Directivity as a function of the beam's zenith angle. The plot is produced by PLOT_MAXGAIN.M, based on Eq. (71) and the simplified element gain of Eq. (73), with assumed element directivity $G_e = 11.5$ dBi, and element zenith angle $\theta = 35°$. The dark portion of the curve corresponds to directivity that is at most 3 dB below the reference directivity $G_{ref} = 48 \times G_e = 28.3$ dBi. The bottom panel gives the half power beam width in the vertical plane. The markers in the top panel are at zenith angles 13.0°, 20.0°, 35.0°and 60.1°, corresponding to common volume altitudes 1000 km, 600 km, 300 km and 120 km. The directivities in these directions are 26.1 dBi, 28.7 dBi, 28.1 dBi and 25.4 dBi. The plot was produced by PLOT_MAXGAIN.M.

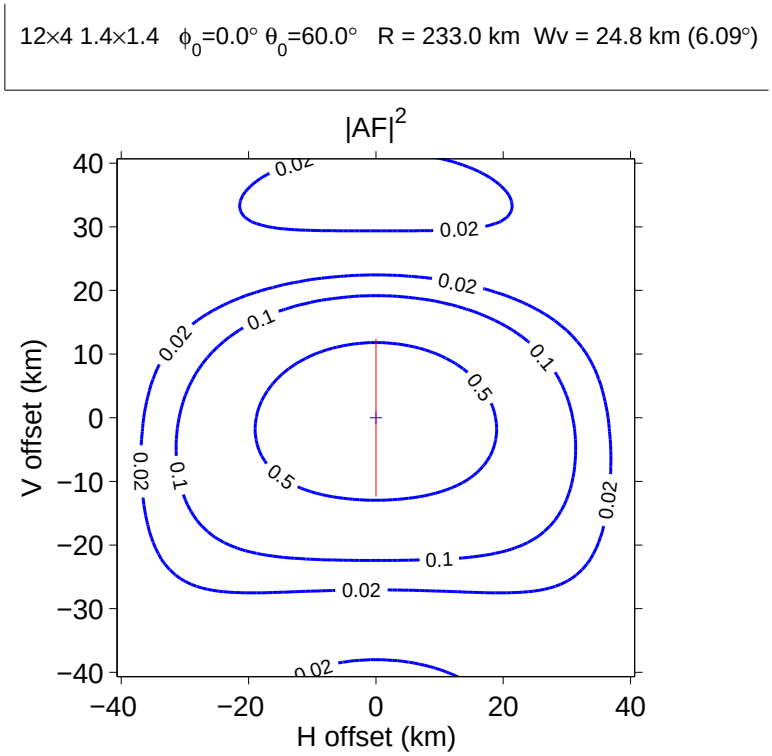

Figure 27: TA: Receiver beam perpendicular cross section through the center of the common volume, at 120 km altitude above the VHF antenna, at the distance of 233 km from the test array. Beam elevation is 30°. The contours give the relative gain $g = |\mathrm{AF}|^2$, normalized to unity at the beam center. The half-power vertical beam width (red line) is 6.1°. The plot was produced by BEAMSHAPE2D.M.

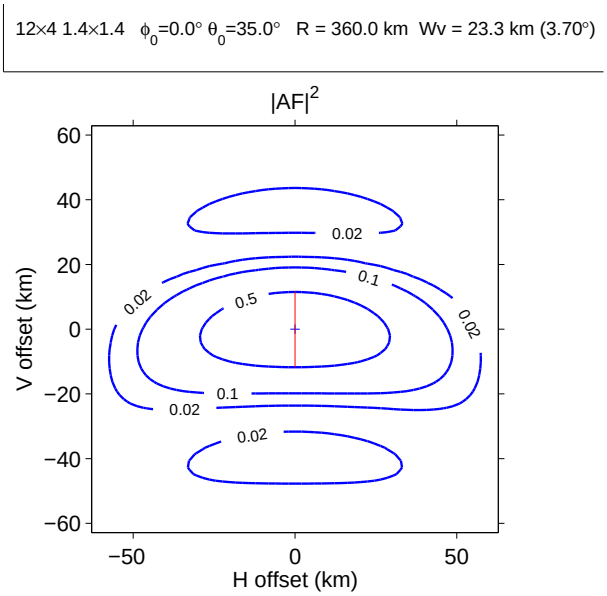

Figure 28: TA: Receiver beam perpendicular cross section through the center of the common volume, at 300 km altitude above the VHF antenna, at the distance of 360 km from the test array. Beam elevation is 55°. The half-power beam width (red line) is 3.70°.

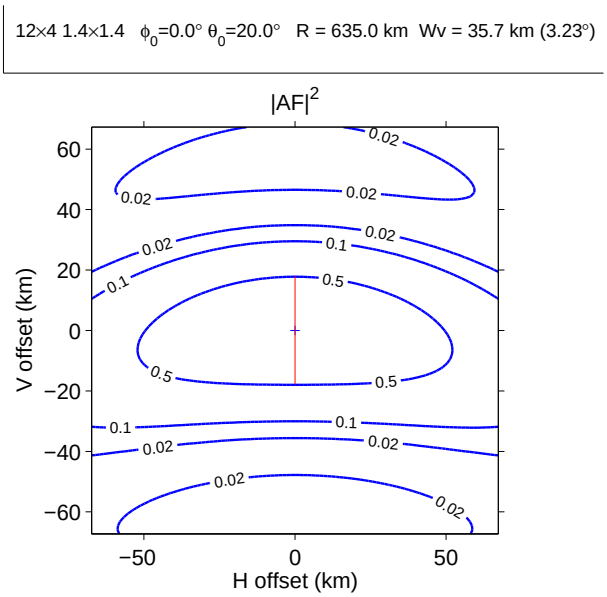

Figure 29: TA: Receiver beam perpendicular cross section through the center of a common volume at 600 km altitude. The beam elevation is 70°, and the range to the center of the common volume is 635 km. Beam elevation is 70°. The half-power beam width (red line) is 3.23°.

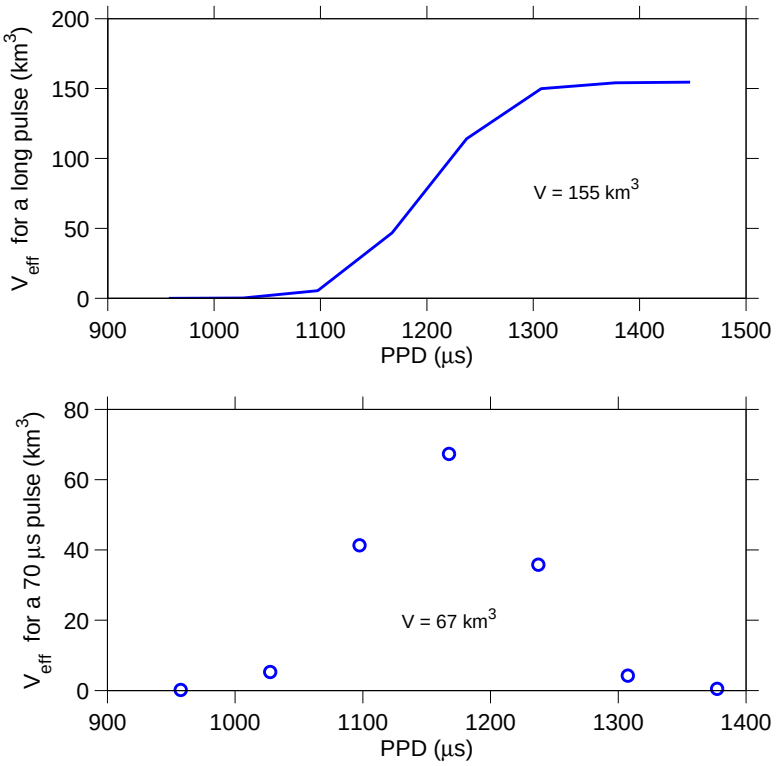

Figure 30: TA: Filling of the common volume at about 120 km altitude. The top panel shows how the common volume fills as a function of the propagation time of a long, volume-filling, pulse. For instance, the signal that is received at about 1400 μs after the start of transmission, comes from the whole 155 km^3 common volume. The curve at the bottom panel gives the effective scattering volume as function of time for a 70 μs pulse. Such a pulse is never able to illuminate the whole volume, so the maximal scattering volume is less than the size of the common volume. The plots are produced by COMMON_VOLUME.M.

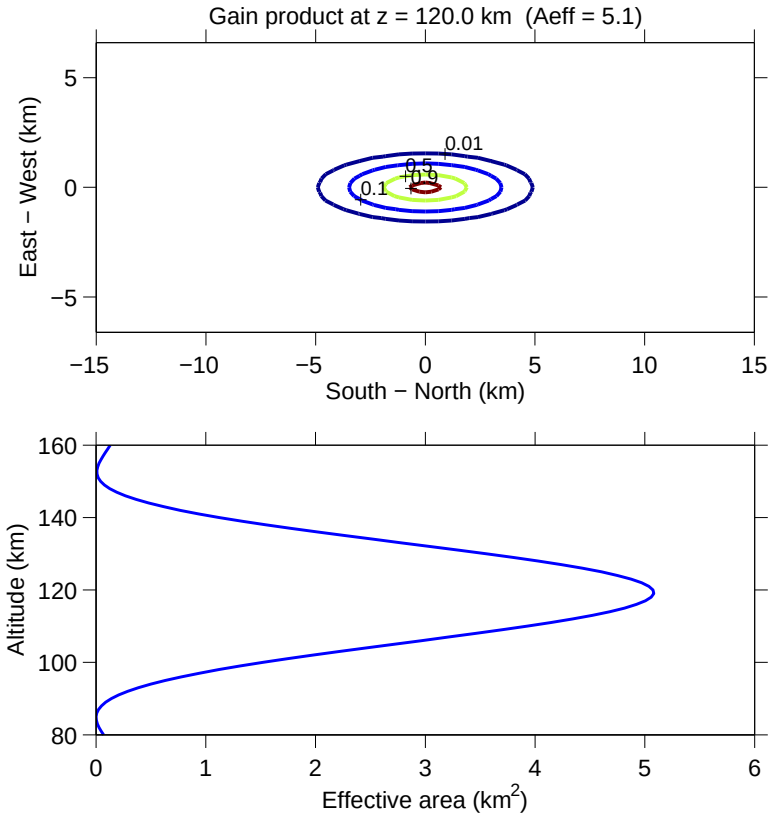

Figure 31: TA: Horizontal slices through the common volume at about 120 km altitude. In the top panel, the curves are contours of the quantity Γ, defined in Eq. (96), at the nominal beam intersection altitude. The bottom panel gives the effective are, defined in Eq. (97), as a function of altitude. The plot was produced by COMMON_VOLUME.M.

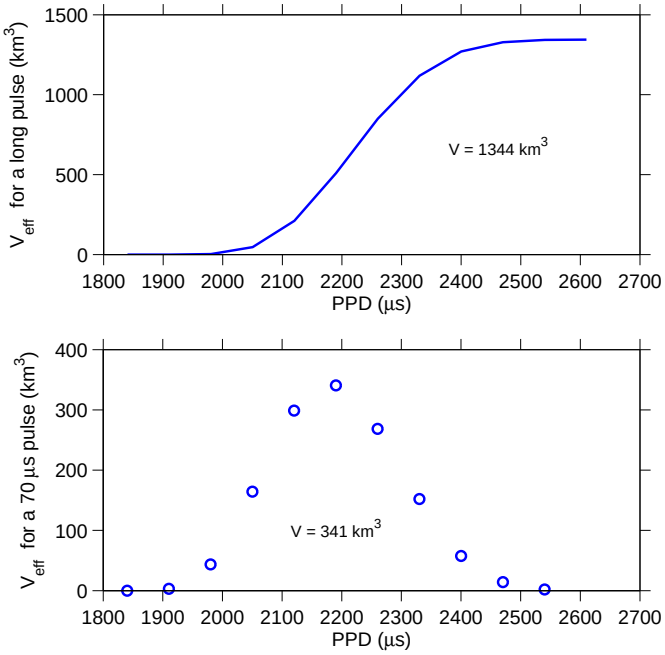

Figure 32: TA: Filling of the common volume at 300 km altitude.

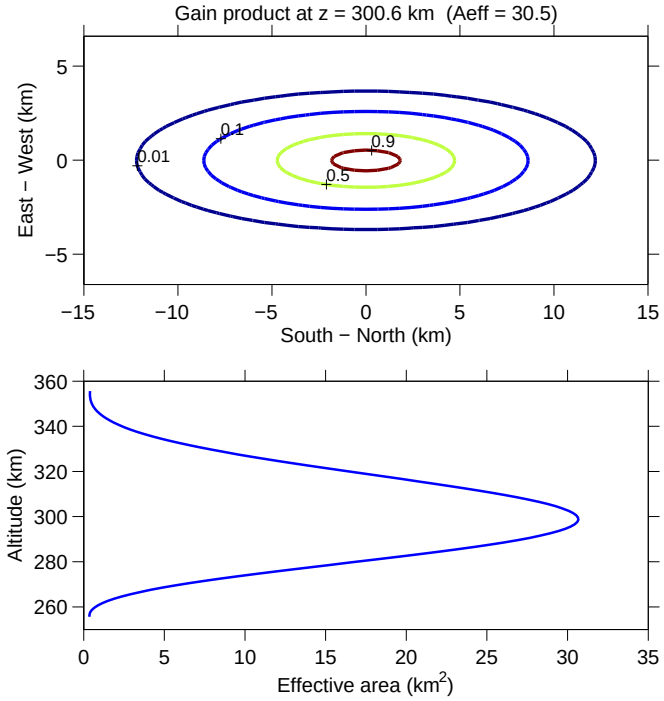

Figure 33: TA: Horizontal slice through the common volume at 300 km altitude. The curves are contour curves of the "relative gain" Γ, defined in Eq. (96).

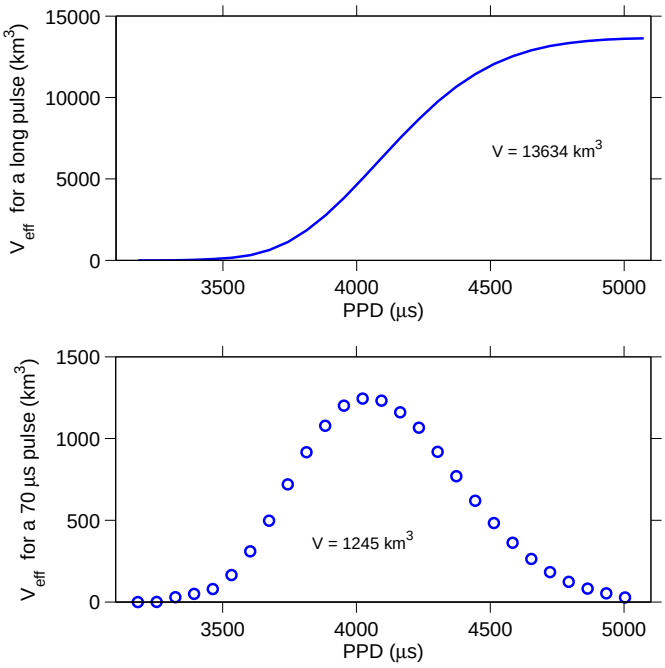

Figure 34: TA: Filling of the common volume at 600 km altitude.

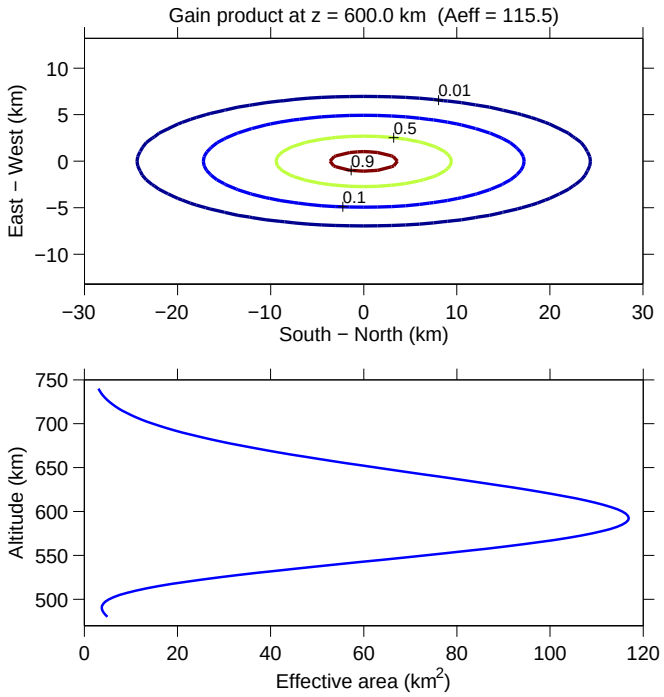

Figure 35: TA: Horizontal slice through the common volume at 120 km altitude.

B. Pointing geometry

The function SITEGEOM1.M computes and plots elevation, azimuth, range and the beam intersection angle χ at the specified site, for Tromsø vertical, field-aligned and CP2 pointing schemes. The pointing info for several prospective and current sites are shown Fig. 36–41. The program calls the official EISCAT geometry package GEOM (standard EISCAT filesystem location `/kst/eros4/geom`) to perform the geometry computations, so this directory must be on the Matlab path. The package has been modified to allow the standard EISCAT ESR site to be *replaced* by an arbitrary site. The geometry package version 1.4 or higher contains these modifications.

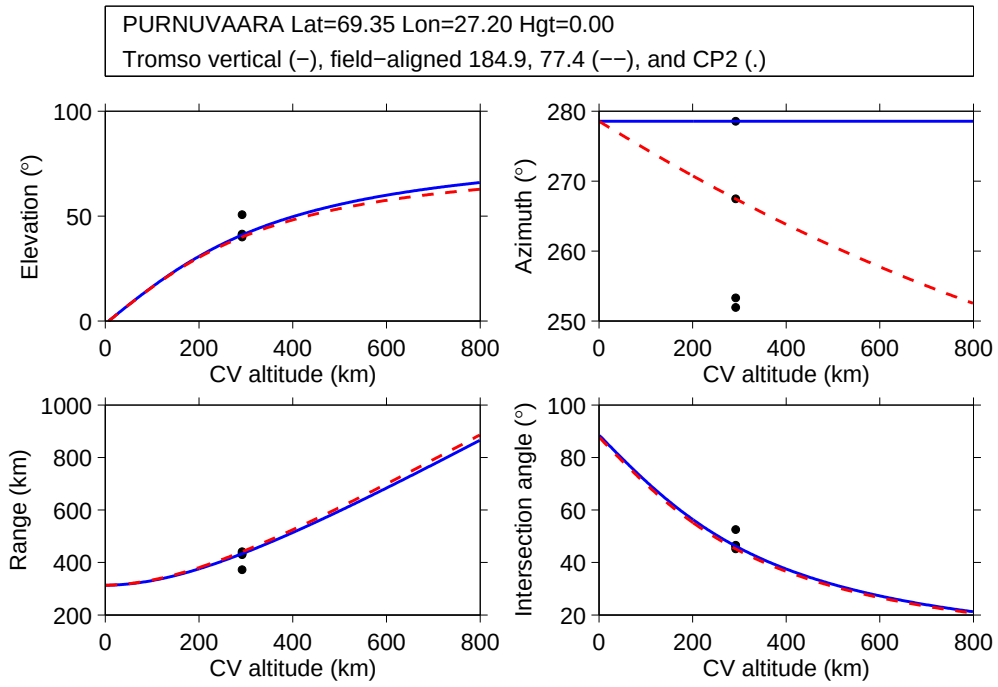

Figure 36: Pointing directions from Purnuvaara to Tromsø.

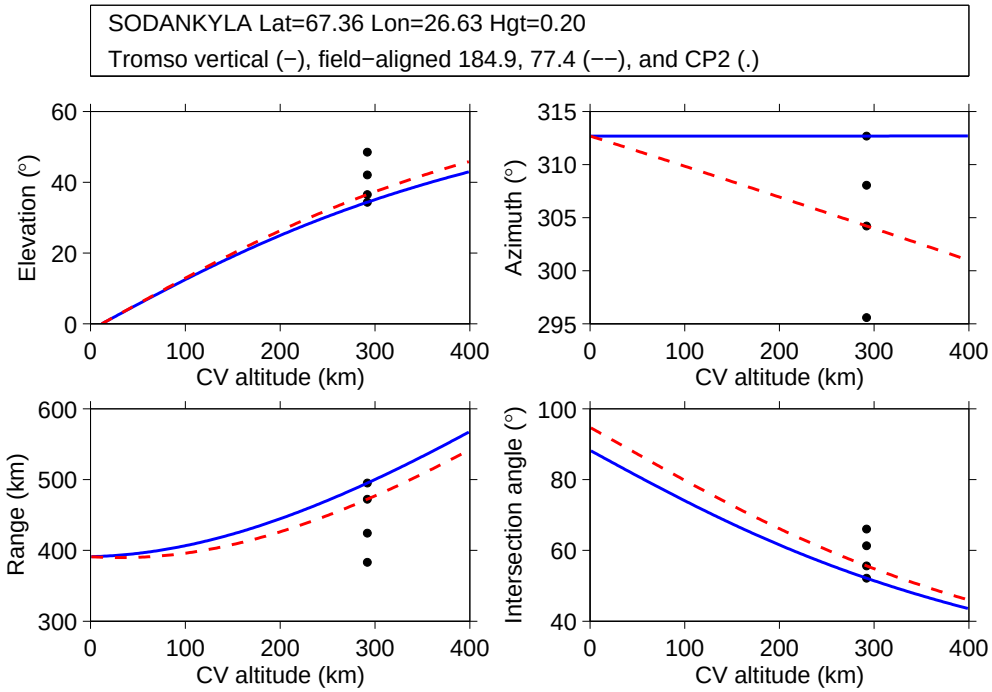

Figure 37: Pointing directions from Sodankylä.

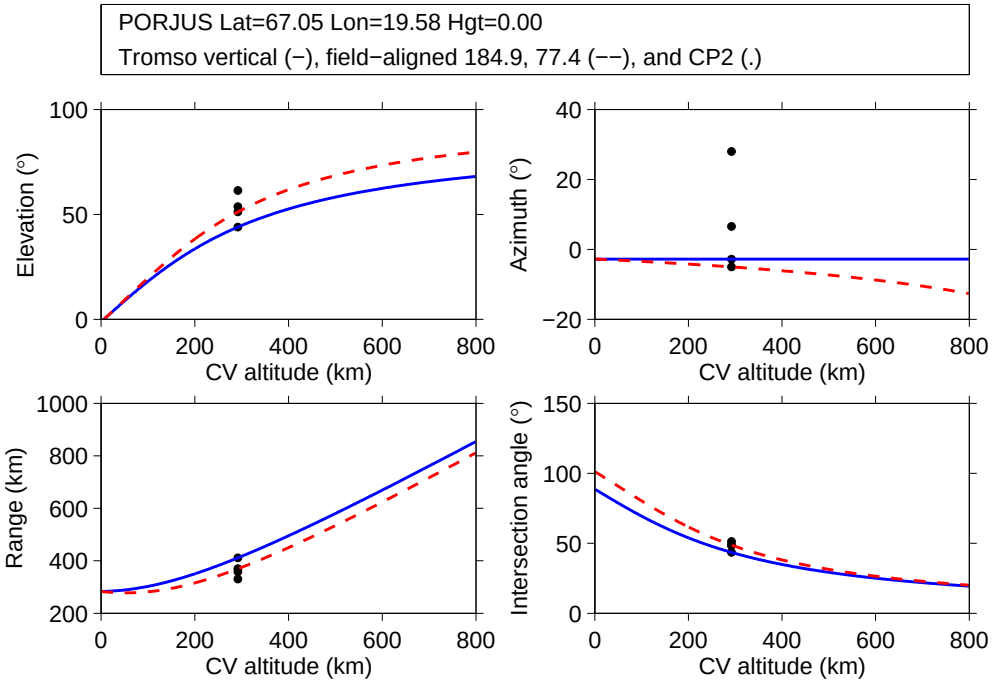

Figure 38: Pointing directions from Porjus.

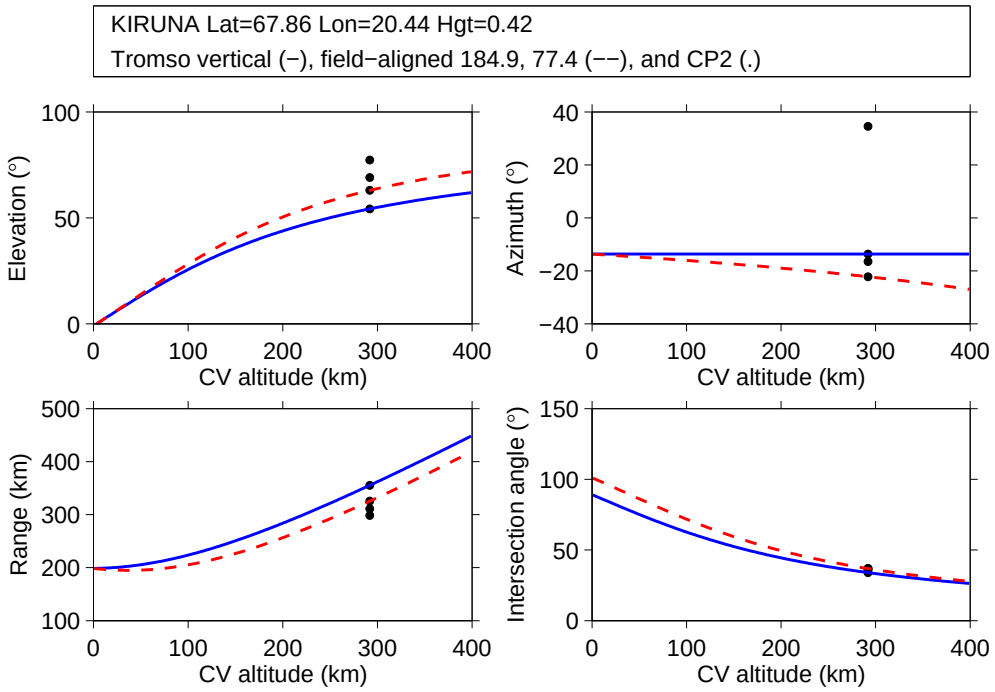

Figure 39: Pointing directions from Kiruna.

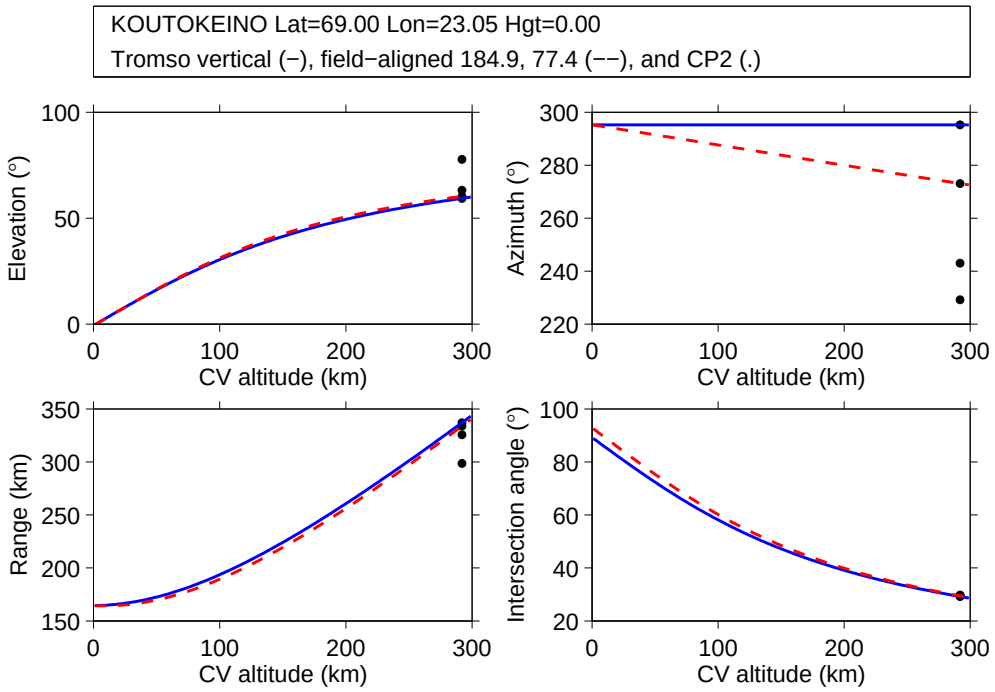

Figure 40: Pointing directions from Koutokeino.

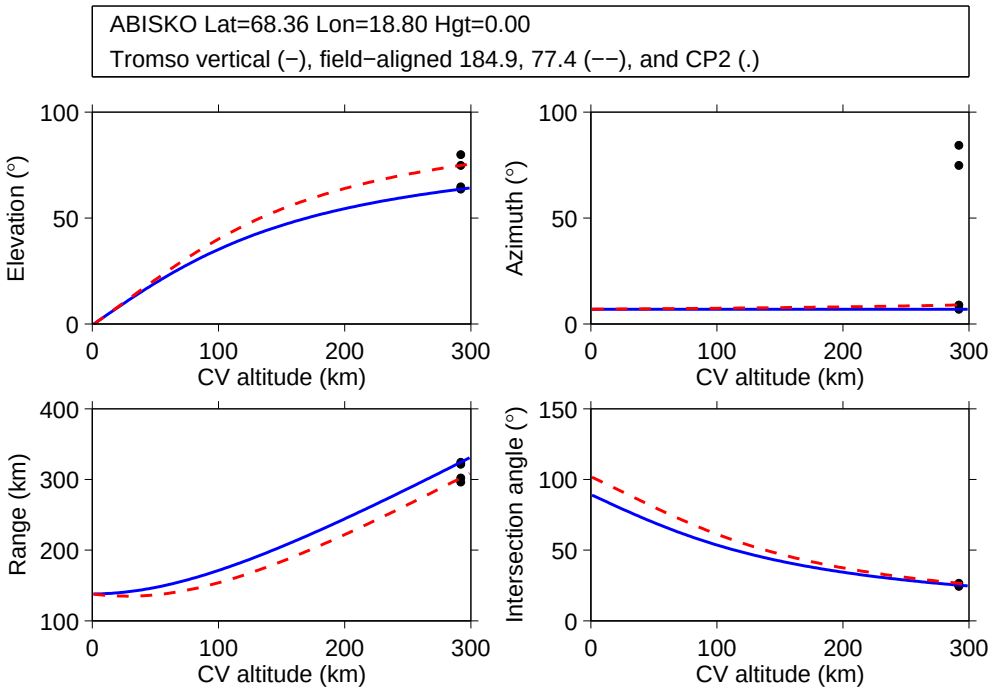

Figure 41: Pointing directions from Abisko.

C. Matlab functions

There are two types of m-files in the e3ant directory: m-files that produce plots, and m-files that don't. The plotting files have simple headers and do not usually allow parameter input on the command line. Instead, they require that the input parameters be hardcoded in the files themselves. Plotting normally requires so much parameters and fine-tuning that putting all that info into call parameter list is impractical. Thus, the files must be manipulated, but I have made an effort to indicate what can be safely modified. The other group of m-files perform some clearly defined computation and have normal parametrized headers, and the normal Matlab help should work usefully in their case.

Plotting functions

- BEAMSHAPE2D — Plot beam's 2D cross section.
- BEAMSTEERING — Plot beam direction as a function of phasing angle.
- COMMON_VOLUME — Compute and plot the size of the effective scattering volume.
- PLANEARRAY — Plot array gain in V-plane at any azimuth.
- PLANEARRAY-JITTER — Plot beam shape jitter distributions.
- PLOT_MAXGAIN — Plot maximum available gain (the element's gain) and the vertical beamwidth as function of elevation.
- SIMPLEBEAM — Plot the $cos^n(\theta/2)$ gain pattern.
- SITEGEOM1 — Plot a sites's pointing directions for certain Tromsø beam directions.

Computation-only functions

- ARRAYGAIN Compute array factor and element gain in arbitrary directions.
- BEAMWIDTH Compute vertical beam width of an array.
- GRATING_DIR Compute an array's grating beam directions.
- POWERINT Computes an array's directivity and power integral.
- SIMPLEGAIN Compute an element's normalized gain assuming $\cos^n(\theta/2)$ shape.
- SIMPLE_VHFBEAM Gaussian approximation to VHF antenna beam shape.
- TESTARRAY_SNR Compute the expected SNR for the test array.